



A LREE-depleted component in the Afar plume: Further evidence from Quaternary Djibouti basalts

Mohammed Daoud, René Maury, Jean-Alix Barrat, R. E. Taylor, Bernard Le Gall, Hervé Guillou, Joseph Cotten, Joël Rolet

► To cite this version:

Mohammed Daoud, René Maury, Jean-Alix Barrat, R. E. Taylor, Bernard Le Gall, et al.. A LREE-depleted component in the Afar plume: Further evidence from Quaternary Djibouti basalts. *Lithos*, Elsevier, 2010, 114 (3-4), pp.327-336. <10.1016/j.lithos.2009.09.008>. <insu-00465553>

HAL Id: insu-00465553

<https://hal-insu.archives-ouvertes.fr/insu-00465553>

Submitted on 24 Feb 2011

HAL is a multi-disciplinary open access archive for the deposit and dissemination of scientific research documents, whether they are published or not. The documents may come from teaching and research institutions in France or abroad, or from public or private research centers.

L'archive ouverte pluridisciplinaire **HAL**, est destinée au dépôt et à la diffusion de documents scientifiques de niveau recherche, publiés ou non, émanant des établissements d'enseignement et de recherche français ou étrangers, des laboratoires publics ou privés.

1 A LREE-depleted component in the Afar plume: further 2 evidence from Quaternary Djibouti basalts

3
4

Mohamed A. Daoud ^{a,b}, René C. Maury ^{a*}, Jean-Alix Barrat ^{a5}, Rex N.
Taylor ^c, Bernard Le Gall ^a, Hervé Guillou ^d, Joseph Cotten ^a, Joël Rolet ^{a 6}

7
8

^a9 *Université Européenne de Bretagne, Université de Brest; CNRS; UMR 6538 Domaines Océaniques;*

10 *Institut Universitaire Européen de la Mer, Place N. Copernic, 29280 Plouzané, France.*

^b11 *Centre d'Etudes et de Recherches Scientifiques de Djibouti, B.P. 486, Djibouti.*

^c12 *School of Ocean and Earth Science, NOC, University of Southampton, Southampton SO14 3ZH, UK.*

^d13 *UMR 1572 LSCE/CEA-CNRS, Domaine du CNRS, 12 avenue de la Terrasse, 91118 Gif-sur-Yvette,
14 France.*

15

16 * Corresponding author. Tel.: (33)298498708; fax: (33)298498760

17 *E-mail address:* maury@univ-brest.fr

18

19 **Abstract**

20

21 Major, trace element and isotopic (Sr, Nd, Pb) data and unspiked K-Ar ages are presented for Quaternary
22 (0.90-0.95 Ma old) basalts from the Hayyabley volcano, Djibouti. These basalts are LREE-depleted ($L_{an}/S_{m}n =$
0.76-0.83), with $^{87}Sr/^{86}Sr$ ratios ranging from 0.70369 to 0.70376, and rather homogeneous $^{143}Nd/^{144}Nd$ ($Nd =$
 $+5.9 - +7.3$) and Pb isotopic compositions ($^{206}Pb/^{204}Pb = 18.47-18.55$, $^{207}Pb/^{204}Pb = 15.52-15.57$, $^{208}Pb/^{204}Pb =$
25 38.62-38.77). They are very different from the underlying enriched Tadjoura Gulf basalts, and from the N26
MORB erupted from the nascent oceanic ridges of the Red Sea and Gulf of Aden. Their compositions closely
27 resemble those of (1) depleted Quaternary Manda Hararo basalts from the Afar depression in Ethiopia and (2)
28 one Oligocene basalt from the Ethiopian Plateau trap series. Their trace element and Sr, Nd, Pb isotope
29 systematics suggest the involvement of a discrete but minor LREE-depleted component, which is probably an
30 intrinsic part of the Afar plume.

31

32 **1. Introduction.**

33

34 The study of basalts from intra-oceanic islands and plateaus as well as from traps and
35 rifts has shown the considerable chemical heterogeneity of plume materials (Hart, 1988). This

36 heterogeneity might indicate very complex plume structures and dynamics (Lin and van
37 Keken, 2006). However, it may not only result from the initial chemical heterogeneity of
38 mantle plumes at depth but also from the entrainment of surrounding mantle materials (Hart et
39 al., 1992; Furman et al., 2006). In addition, a lithospheric component is clearly recognized in
40 some intracontinental basalts, e.g. in the Afar province, but its origin is still debated (Rogers,
41 2006). Some authors have suggested that melting of the Afar lithospheric mantle explains a
42 significant proportion of the erupted lavas (Hart et al., 1989; Vidal et al., 1991; Deniel et al.,
43 1994) whilst others point out that continental crust contamination can also contribute to the
44 isotopic signature of these basalts (Barrat et al., 1993; Baker et al., 1996; Pik et al., 1999).

45 The vast majority of plume-related basalts, including the Afar ones (Furman et al., 2006;
46 Beccaluva et al., 2009) are dominated by a component that is chemically and isotopically
47 enriched. However, the occurrence of subordinate components characterized by a light rare
48 earth element (LREE) depletion has been suggested from the study of basalts from major
49 mantle plumes in: (1) Iceland (Zindler et al., 1979; Hémond et al., 1993; Taylor et al., 1997;
50 Chauvel and Hémond, 2000; Skovgaard et al., 2001; Fitton et al., 2003; Thirlwall et al., 2004;
51 Kokfelt et al., 2006); (2) Hawaii (Chen and Frey, 1985; Yang et al., 2003; Frey et al., 2005);
52 (3) the Galapagos (White et al., 1993; Hoernle et al., 2000; Blichert-Toft and White, 2001;
53 Saal et al., 2007); and (4) the Kerguelen Archipelago (Doucet et al., 2002). However, the
54 characterization of this reservoir is difficult because its signature may be overprinted by either
55 the dominant enriched plume component or the lithospheric reservoirs. Therefore, the
56 presence of an intrinsic depleted component in plumes is still an open question.

57 LREE-depleted basalts associated to the Afar mantle plume have long been recognized
58 in the Quaternary Manda Hararo volcanic chain, Ethiopia (Treuil and Joron, 1975; Joron et
59 al., 1980; Barrat et al., 2003). A single LREE-depleted Oligocene Ethiopian Plateau basalt has
60 also been so far analysed (sample E88: Pik et al., 1998, 1999). The purpose of this paper is:
61 (1) to describe another newly discovered occurrence of such basalts in the SE part of the Afar
62 triangle, i.e. the rather large Hayyabley Quaternary volcano in Djibouti (Fig. 1), and (2) to
63 discuss its bearing on the composition and heterogeneity of the Afar mantle plume.

64

65 **2. Analytical techniques**

66

67 Ar isotopic compositions and K contents (Table 1) were measured at Gif-sur-Yvette and
68 IUEM (Institut Universitaire Européen de la Mer), respectively. The samples were crushed,
69 sieved to 0.25-0.125 mm size fraction and ultrasonically washed in acetic acid. Potassium and

70 argon were measured on the microcrystalline groundmass, after removal of phenocrysts using
71 heavy liquids of appropriate densities and magnetic separations. This process improves the K
72 yield as well as the percentage of radiogenic argon, and removes at least some potential
73 sources of systematic error due to the presence of excess ^{40}Ar in olivine and feldspar
74 phenocrysts (Laughlin et al., 1994). Ar analyses were performed using the procedures detailed
75 in Yurtmen et al. (2002) and Guillou et al. (2004). The unspiked technique differs from the
76 conventional isotope dilution method in that argon extracted from the sample is measured in
77 sequence with purified aliquots of atmospheric argon at the same working gas pressure in the
78 mass-spectrometer. This suppresses mass discrimination effects between the atmospheric
79 reference and the unknown, and allows quantities of radiogenic $^{40}\text{Ar}^*$ as small as 0.14% to be
80 detected on a single-run basis (Scaillet et al., 2004). Argon was extracted by radio frequency
81 heating of 2.0 – 3.0 g of sample, then transferred to an ultra-high-vacuum glass line and
82 purified with titanium sponge and Zr-Ar getters. Isotopic analyses were performed on total
83 ^{40}Ar contents ranging between 2.4 and 3.2×10^{-11} moles using a 180°, 6 cm radius mass
84 spectrometer with an accelerating potential of 620V. The manometric calibration (Charbit et
85 al., 1998) was based on periodic, replicate determinations of international dating standards
86 including LP-6 (Odin et al., 1982) and HD-B1 (Fuhrmann et al., 1987). The total ^{40}Ar content
87 of the sample can be determined with a precision of $\pm 0.2\%$ (2σ) according to this procedure.
88 Ages were calculated using the constants recommended by Steiger and Jäger (1977).

89 Major element compositions of minerals and glasses were determined using a Cameca
90 SX50 five spectrometer automated electron microprobe (Microsonde Ouest, Plouzané,
91 France). Analytical conditions were 15 kV, 10-12 nA and a counting time of 6 sec. (see
92 Defant et al., 1991, for further analytical details). Major and trace element data on bulk rocks
93 (Table 2) were first obtained by Inductively Coupled Plasma-Atomic Emission Spectrometry
94 (ICP-AES) at IUEM, Plouzané. The samples were finely powdered in an agate grinder.
95 International standards were used for calibration tests (ACE, BEN, JB-2, PM-S and WS-E).
96 Rb was measured by flame emission spectroscopy. Relative standard deviations are $\pm 1\%$ for
97 SiO_2 , and $\pm 2\%$ for other major elements except P_2O_5 and MnO (absolute precision $\pm 0.01\%$),
98 and ca. 5% for trace elements. The analytical techniques are described in Cotten et al. (1995).
99 Concentrations of additional trace elements were measured by Inductively Coupled Plasma
100 Mass Spectrometry (ICP-MS) at IUEM, using a Thermo Element 2 spectrometer following
101 procedures adapted from Barrat et al. (1996, 2000). Based on standard measurements and
102 sample duplicates, trace element concentration reproducibility is generally better than 5 %
103 (Barrat et al., 2007), and are in good agreement with the ICP-AES results (Table 2).

104 Isotopic compositions of Sr and Nd (Table 4) were determined at IUEM. Conventional
105 ion exchange techniques were used for separation of Sr, and isotope ratio measurements were
106 carried out by thermal ionization mass spectrometry using a Thermo Triton equipped with 7
107 collectors. Isotopic ratios were normalized for instrumental mass fractionation relative to
108 $^{86}\text{Sr}/^{88}\text{Sr} = 0.1194$. $^{87}\text{Sr}/^{86}\text{Sr}$ of the NBS 987 Sr standard yielded 0.710213 ± 22 (2σ , $n=14$) and
109 the sample Sr isotopic compositions are reported relative to $^{87}\text{Sr}/^{86}\text{Sr} = 0.71024$. The Nd
110 purification was done according to the procedure described in Dosso et al. (1993). TRU Spec
111 chromatographic resins from Eichrom were used to separate the REE fraction from the sample
112 matrix. Then, the separation and elution of Nd and other REE were realized on Ln.Spec resin.
113 During the course of the study, analyses of the La Jolla standard were performed and gave an
114 average of $^{143}\text{Nd}/^{144}\text{Nd} = 0.511845 \pm 6$ ($n=15$). All Nd data were fractionation-corrected to
115 $^{146}\text{Nd}/^{144}\text{Nd} = 0.7219$ and further normalized to a value of $^{143}\text{Nd}/^{144}\text{Nd} = 0.511860$ for the La
116 Jolla standard.

117 Isotopic compositions of Pb were determined at the National Oceanography Centre,
118 Southampton, using the SBL 74 double spike. Powdered samples were leached with 6 M HCl
119 at 140°C for 1 hour and then rinsed up to 6 times with ultrapure water prior to dissolution.
120 Lead separation was then performed on an anionic exchange resin. High-resolution Pb
121 isotopic analyses were carried out on a VG sector 54 multi-collector instrument, using the
122 double spike technique with the calibrated Southampton-Brest $^{207}\text{Pb}/^{204}\text{Pb}$ spike (Ishizuka et
123 al., 2003). The true Pb isotopic compositions were obtained from the natural and mixture runs
124 by iterative calculation adopting a modified linear mass bias correction (Johnson and Beard,
125 1999). The reproducibility of this Pb isotopic measurement (external error: 2σ) by double
126 spike is < 200 ppm for all $^{20x}\text{Pb}/^{204}\text{Pb}$ ratios. Measured values for NBS SRM-981 during the
127 measurement period were $^{206}\text{Pb}/^{204}\text{Pb} = 16.9414 \pm 26$, $^{207}\text{Pb}/^{204}\text{Pb} = 15.4997 \pm 30$ and
128 $^{208}\text{Pb}/^{204}\text{Pb} = 36.726 \pm 9$ (2σ , $n = 9$). Pb blanks measured using this procedure were < 100 pg,
129 and thus negligible relative to the amount of sample analysed.

130
131

132 **3. Geological setting and K-Ar ages**

133

134 *3.1. Geological and tectonic framework*

135

136 The geology of the Republic of Djibouti records the effects of the activity of the Afar
137 mantle plume since 30 Ma (Schilling, 1973; Barberi et al., 1975; Barberi and Varet, 1977;

138 Furman et al., 2006). Plume-related basaltic and derived magmas, variably enriched in
139 incompatible elements (e.g., Joron et al., 1980; Deniel et al., 1994) cover ca. 90% of its
140 surface, and range in age from at least 23.6 ± 0.5 Ma to Present (Barberi et al., 1975;
141 Courtillot et al., 1984; Zumbo et al., 1995). Since the Miocene, the most salient tectono-
142 magmatic process observed in the area was the penetration of the Gulf of Aden (GA) oceanic
143 ridge between the Arabia and Somalia plates, hence leading to the opening of the Tadjoura
144 Gulf (Courtillot et al., 1980; Manighetti et al., 1997), at the southwestern edge of which the
145 emerged Asal Rift shows spectacular evidence for both tectonic and magmatic activities
146 (Stieltjes et al., 1976; Needham et al., 1976).

147 Onland, the principal marker of the Pliocene opening of the Tadjoura Gulf (TG) was the
148 emplacement of a < 350 m-thick basaltic lava flow pile, referred to as the “initial basaltic
149 series from the borders of the Tadjoura Gulf” (Fournier et al., 1982; Gasse et al., 1983), which
150 will be named hereafter the Tadjoura Gulf Basalts (TGB). These very fluid subaerial lava
151 flows are generally assumed to have been emitted from now submerged fissures in the Gulf,
152 and emplaced rather symmetrically outwards on the twin margins (Fig. 1, inset) (Richard,
153 1979). Additional feeder dykes, and associated neck-like features, have been identified
154 onshore, along the northern flank in the Tadjoura area. TGB range from olivine tholeiites to
155 ferrobasalts, and in thin section are subaphyric to sparsely phyric, with 3-6 modal% calcic
156 plagioclase, and 1-3 modal% olivine set in a microlitic groundmass. They display mild, but
157 significant, enrichments in light rare earth elements (LREE) and other highly incompatible
158 elements (Joron et al., 1980; Barrat et al., 1990, 1993; Deniel et al., 1994).

159 In the Djibouti plain, the TGB are involved in a coastal network of Gulf-parallel tilted
160 fault blocks, bounded by dominantly extensional N-facing structures, in association with
161 N140°E normal faults outlined by a swarm of small cinder cones (Fig. 1). To the East, they
162 are post-dated by the Hayyabley elongated volcano, the long axis of which also strikes NW-
163 SE, parallel to the regional fault scarp bounding the eastern coastal plain further SE.

164

165 *3.2. The Hayyabley volcano*

166

167 The youngest volcanic units in the Djibouti plain are a set of generally small (less than
168 100 m high) ash and cinder strombolian-type cones with associated basaltic flows (e.g. the
169 Nagâd volcano, Fig. 1), aligned along a young NNW-SSE fracture network (Fournier et al.,
170 1982). They overlie the TGB and have been dated to 1.75-1.70 Ma (Gasse et al., 1983). The
171 largest of these post-TGB volcanic centers is the Hayyabley volcano, east of Djibouti town

172 (Fig. 1). Although it was shown on the 1:50 000 geological map of Djibouti (Fournier et al.,
173 1982), and further well-described and dated by Gasse et al. (1983), it was apparently never
174 investigated later despite the obviously unusual characteristics of its basaltic lavas.

175 The Hayyabley volcano in map-view is a 5x10 km elliptic edifice, with a NNW-SSE
176 trending axis. It has a shield-like and rather flat morphology, and culminates at 147 m at
177 Signal Bouêt. It overlies the TGB lava flows outcropping W and N of Wadi Ambouli valley
178 (Fig. 1), and seals the EW to WNW-ESE normal fault pattern related to the Tadjoura rift.
179 Despite the rather large aerial extent of its lavas, we estimate its volume to ca. 0.6-0.8 km³
180 only. Its eruptive vents are no longer identifiable, possibly because of the strong anthropic
181 imprint and constructions of the Djibouti suburbs: they are thought to be located in its summit
182 zone, and aerial photograph data suggest radial emplacement of the lava flows away from this
183 summit (Fournier et al., 1982).

184 The total thickness of the Hayyabley lava flow pile is estimated at 120 m. The best
185 section is exposed in Wadi Warabor, along the northern coast (Fig. 1). There, we sampled
186 seven superimposed basaltic lava flows (DJ54B to DJ54H), resting conformably upon a 15 m-
187 thick columnar-jointed lava flow (DJ54A) belonging to the TGB sequence. These flows are
188 vesicle-rich, and their thickness decreases upwards from ca. 4 m to less than 20 cm. Only the
189 thickest lava flows show columnar jointing, and the uppermost ones are highly vesicular and
190 often scoriaceous (Gasse et al., 1983). A sample (TF 914) collected from a possible eruption
191 vent in the summit area had been dated by the K-Ar unspiked method to 0.98 ± 0.10 Ma and
192 0.83 ± 0.08 Ma (Gasse et al., 1983), the youngest K-Ar dates obtained so far in the area. We
193 have checked the previous results by dating two basaltic flows from the Wadi Warabor
194 section (Fig. 1). The results are shown in Table 1. The two ages obtained, 0.93 ± 0.06 Ma and
195 1.06 ± 0.09 Ma, are mutually consistent, and compatible as well with those previously
196 published (Gasse et al., 1983). Indeed, the four results almost overlap at around 0.91 – 0.97
197 Ma, and are remarkably convergent considering the very low concentration of potassium in
198 the studied samples and the young age range.

199

200

201 **4. Petrologic and geochemical results**

202

203 *4.1. Petrographic and mineralogical features*

204

205 The Hayyabley basalts are rather homogeneous from a petrographic point of view, and
206 also quite different from the underlying TGB. They are moderately to highly vesicular (10 to
207 30 modal% vesicles in thin section). These vesicles are usually empty, or sometimes partly
208 filled by calcite, especially in the summit part of the volcano. The rocks are also sparsely to
209 moderately phyrlic, with 5 to 15 modal% phenocrysts, the size of which ranges from 0.5 to 3
210 mm. They include olivine (dominant) and calcic plagioclase (subordinate), in a roughly 2:1
211 ratio. These phenocrysts are set in a holocrystalline groundmass, showing doleritic or
212 intersertal textures. It contains, by order of decreasing abundance, plagioclase laths, olivine
213 microcrysts (the periphery of which is often replaced by iddingsite), calcic pyroxene grains
214 and titanomagnetite.

215 Olivine compositions range from Fo₈₄₋₈₂ for the phenocryst cores to Fo₇₈₋₅₄ for their rims
216 and the microcrysts, the smallest ones being the most Fe-rich. The plagioclase phenocryst
217 cores are bytownitic (An₈₆₋₇₇) and contain negligible amounts of Or component (<0.3%). The
218 corresponding rims are less calcic (An₇₀₋₃₂) and the small laths from the groundmass are
219 clearly enriched in alkalis (up to An₂₇₋₁₅ Ab₇₀₋₈₀ Or₂₋₅). Groundmass clinopyroxenes are augitic
220 (Wo₄₅₋₄₁ En₄₃₋₄₀ Fs₁₂₋₁₆) and their low TiO₂ (<1 wt%) and Na₂O (<0.3 wt%) contents are
221 typical of tholeiitic clinopyroxenes.

222

223 *4.2. Major and trace elements on bulk rocks*

224

225 Nine samples taken from different flows from four locations (Fig. 1) were analysed, and
226 the results are given in Table 2. Their major and trace element abundances are rather uniform.
227 These lavas display high Al₂O₃ (16.4-17.05 wt%) and CaO (12.5-13.8 wt%) abundances, low
228 Na₂O (1.9-2.1 wt%) abundances and FeO*/MgO ratios close to 1. Although not primitive,
229 these lavas are amongst the least evolved basalts collected so far from the Republic of
230 Djibouti. Indeed, they exhibit the highest compatible trace element abundances (e.g., Ni, Co,
231 Cr) measured in samples from this area (e.g., Joron et al., 1980; Barrat et al., 1990, 1993;
232 Deniel et al., 1994).

233 More importantly, their incompatible trace element abundances are low, and these
234 samples are characterized by light REE depletions (La_n/Sm_n=0.76-0.83), and small but
235 significant positive Eu anomalies (Eu/Eu*=1.08-1.12, Fig. 2). These features unambiguously
236 distinguish the Hayyabley basalts from both the TGB and the older post-TGB basalts, which
237 are always LREE-enriched (Joron et al., 1980; Barrat et al., 1990, 1993; Deniel et al., 1994).

238 The unusual features of the Hayyabley basalts are strengthened by their primitive mantle
239 normalised patterns that exhibit large positive Ba ($Ba_n/Rb_n=2.9-8.6$) and Sr ($Sr_n/Ce_n=1.8-2.1$)
240 anomalies (Fig. 3). Although LREE-depleted, the Hayyabley basalts are clearly distinct from
241 typical N-MORB and basalts erupted by the nearby nascent oceanic ridges. For example,
242 basalts with N to T-MORB affinities are known from the eastern part of the Tadjoura Gulf
243 (Barrat et al., 1990, 1993). Although a positive Sr anomaly has been observed in a single
244 LREE-depleted basalt, positive Ba and Eu anomalies are missing (Barrat et al., 1990, 1993
245 and unpublished results). In addition, the Nb/Y and Zr/Y ratios (0.11-0.15 and 2.20-2.57,
246 respectively, Table 2) of Hayyabley basalts are such that these lavas plot within the field of
247 Icelandic plume basalts, and well above the N-MORB field, in Fitton et al.'s (1997, 2003)
248 rectangular plot (not shown).

249 Interestingly, the Hayyabley basalts are remarkably similar to the scarce LREE-depleted
250 basalts which were sporadically emitted by the Manda Hararo rift, Ethiopia (Barrat et al.,
251 2003). Indeed, the latter display incompatible element abundances and distributions very
252 similar to those of the Hayyabley basalts (Fig. 3). The noticeable differences are minor. The
253 Manda Hararo basalts are somewhat more evolved than the Hayyabley basalts and have for
254 example lower Ni and Cr concentrations (Table 3). In addition, an Oligocene basaltic flow
255 with the same features (sample E88) was reported by Pik et al. (1999) from the Ethiopian
256 Plateau.

257

258 *4.3. Sr, Nd, Pb isotopic data*

259

260 The isotopic compositions of five samples are given in Table 4, and are almost uniform,
261 with the exception of $^{87}Sr/^{86}Sr$ ratios which vary significantly in the range 0.70369 - 0.70396
262 (Table 4). Although relatively fresh, the Hayyabley basalts display some evidence of
263 weathering. One may suspect that their $^{87}Sr/^{86}Sr$ ratios are not pristine, and have been affected
264 by secondary processes. Indeed, the least radiogenic sample DJ59 displays a negative Loss On
265 Ignition (LOI) value (-0.38 wt%). Conversely, the LOI value of the most radiogenic sample
266 (DJ54H) is much higher (0.92 wt%), and in a $^{87}Sr/^{86}Sr$ vs. LOI plot (not shown), a weak
267 positive correlation is apparent. In order to check if the Sr isotopic compositions of the
268 samples were modified by alteration, 150 mg of sample DJ54B was leached for 2 hours in hot
269 (150°C) 6N HCl, and rinsed in deionized water prior to dissolution. Its $^{87}Sr/^{86}Sr$ ratio is
270 significantly lower than the value obtained on the unleached powder (Table 4), a result which

271 suggests that the Sr isotopic compositions have been modified by secondary processes.
272 Similar observations were made by Deniel et al. (1994) on other samples from Djibouti. Thus,
273 $^{87}\text{Sr}/^{86}\text{Sr}$ obtained on unleached samples from this area should be discussed only with extreme
274 caution, even ratios obtained from apparently fresh basalts. We believe that only two $^{87}\text{Sr}/^{86}\text{Sr}$
275 measurements can be safely used in the discussion: the least radiogenic one (DJ59), and the
276 value obtained on the leached residue of DJ54B.

277 The Sr, Nd, and Pb isotopic compositions of the Hayyabley basalts are compared to
278 those of other volcanics from the Horn of Africa in figures 4 to 6. In these plots, Hayyabley
279 basalts lie significantly outside the fields defined by the submarine basalts erupted from the
280 nascent oceanic ridges of the Red Sea, the Eastern part of the Tadjoura Gulf, and the Aden
281 Gulf. These features indicate that these LREE-depleted lavas are unlike MORB (Figs. 5 and
282 6). For example, they display $^{87}\text{Sr}/^{86}\text{Sr}$ ratios more radiogenic than N-MORB, and
283 significantly lower ϵ_{Nd} values (Ito et al., 1987). In contrast, the ϵ_{Nd} vs. $^{87}\text{Sr}/^{86}\text{Sr}$ plot (Fig. 4)
284 shows that the Hayyabley basalts and LREE-depleted basalts from Manda Hararo are
285 isotopically very similar. The Hayyabley basalts display almost uniform Pb isotopic
286 compositions ($^{206}\text{Pb}/^{204}\text{Pb}= 18.47\text{-}18.55$, $^{207}\text{Pb}/^{204}\text{Pb}= 15.52\text{-}15.57$, $^{208}\text{Pb}/^{204}\text{Pb}= 38.62\text{-}38.77$)
287 well above the NHRL (Hart, 1984, 1988; see Table 4). In the Sr-Nd, Pb-Pb and Nd-Pb plots
288 (Figs. 4 to 6), the Hayyabley basalts extend the range of the compositions displayed by the
289 young (< 4 Ma) basalts from Djibouti. They might reflect the contribution of a distinct LREE
290 component in their petrogenesis.

291

292 **5. Discussion**

293

294 Although Ethiopian Plateau basalts (Pik et al., 1999; Kieffer et al., 2004; Meshesha and
295 Shinjo, 2007; Beccaluva et al., 2009), and Afar basalts (Treuil and Joron, 1975; Joron et al.,
296 1980; Deniel et al., 1994) are dominantly enriched, previous studies (Barrat et al., 1993, 2003;
297 Pik et al., 1999; Meshesha and Shinjo, 2007) have demonstrated that minor depleted
298 components were also involved in their petrogenesis. The discovery of a new occurrence of
299 LREE-depleted basalts in Djibouti, i.e. further east in the Afar rift setting, might provide new
300 constrains on their origin. Two main points will be discussed below: (1) the origin of the Ba,
301 Sr and Eu positive anomalies observed in the Hayyabley basalts, and (2) the occurrence of a
302 specific LREE-depleted component in the sources of the Afar basalts.

303

304 *5.1. The Ba, Sr and Eu positive anomalies in the Hayyabley basalts*

305

306 The origin of Ba, Sr and Eu positive anomalies in LREE-depleted basalts has been
307 previously investigated in the cases of some Icelandic basalts (e.g., Kokfelt et al., 2006 and
308 references therein) and of the Manda Hararo basalts (Barrat et al., 2003). The compositions of
309 LREE-depleted basalts such as those erupted by the Hayyabley volcano might be related to
310 those of common MORB. The chief differences between them could be due to secondary
311 processes, such as hot-desert weathering, crystal accumulation, or contamination by a crustal
312 component. Alternatively, they could be derived from an unusual mantle source, located in
313 the lithospheric or asthenospheric mantle or in the plume itself.

314 In a hot-desert environment, surface processes are able to generate positive Ba and Sr
315 anomalies in a very short time. The studies of meteorites from Sahara have demonstrated that
316 some of them, and not only the most weathered ones, exhibit marked Ba and Sr enrichments
317 that are sensitive indicators of the development of secondary calcite, gypsum, or barytes (e.g.,
318 Barrat et al., 1998, 2003). Such processes would have generated a range of Ba and Sr
319 abundances from low values typical of unweathered N-MORB (about 10 ppm Ba and 100
320 ppm Sr) to much higher concentrations. However, Ba and Sr abundances in the Hayyabley
321 basalts are uniform, and strikingly similar to the concentrations measured in the distant
322 Manda Hararo basalts. Furthermore, the development of secondary phases is unable to
323 increase the Eu/Eu* ratio and to generate positive Eu anomalies, hence ruling out this first
324 explanation.

325 Positive Ba, Sr and Eu anomalies in basaltic rocks are usually explained by plagioclase
326 accumulation or assimilation. However this process is unable to produce Sr anomalies as high
327 as those displayed by the Hayyabley or Manda Hararo basalts without increasing drastically
328 the Al₂O₃ contents of the resulting rocks. The fact that the Al₂O₃ abundances of the LREE-
329 depleted basalts are not anomalously high (Table 2) is inconsistent with the hypothesis of
330 plagioclase accumulation. Assimilation of plagioclase-rich gabbros from the oceanic
331 lithosphere during ascent of plume-related magmas has been proposed in the cases of offshore
332 Tadjoura Gulf basalts (Barrat et al., 1993) and Galapagos basalts (Saal et al., 2007). However,
333 reproducing the compositions of Hayyabley basalts through this process, and especially their
334 positive Ba, Sr and Eu anomalies, would require rather high rates of assimilation. In addition,
335 the Hayyabley and Manda Hararo basalts overlie thinned continental crust which is 25-26 km
336 thick (Dugda and Nyblade, 2006), while the depleted plateau basalt sample E88 (Pik et al.,
337 1999) is located on normal (ca. 40 km thick) African crust. Due to the presence of a
338 substantial plume-related basaltic cover in both cases, one may expect the occurrence at

339 crustal or even subcrustal depths of associated gabbroic cumulates. However, these gabbros
340 should be LREE-enriched like the vast majority of Afar basalts. Therefore, their interaction
341 with depleted (N-MORB type) melts is likely to lead to variably LREE-enriched magmas with
342 isotopic compositions close to those of the flood basalts.

343 The Hayyabley basalts have radiogenic Sr isotopic compositions and low ϵNd values
344 relative to Aden Gulf or Red Sea MORBs (Schilling et al., 1992; Volker et al., 1993; Hase et
345 al., 2000). The assimilation of a continental component could explain this shift from usual N-
346 MORB values, but incompatible trace element ratios give no support to this interpretation.
347 Contamination of MORB-like melts by continental crust would produce significant changes in
348 incompatible trace element ratios. The Hayyabley basalts, like the Manda Hararo LREE-
349 depleted basalts, lack the negative Nb or Ta anomalies observed in the multi-element plots of
350 crust-contaminated basalts. Moreover, they show a limited range of Ce/Pb ratios from 24 to
351 28, similar to values measured in oceanic basalts (e.g., Sun and McDonough, 1989).
352 Therefore, there is no indication for assimilation of significant amounts of material derived
353 from the continental crust in the LREE-depleted basalts. In the case of the Manda Hararo
354 basalts, this conclusion is strengthened by their $\delta^{18}\text{O}$ values close to 5.5 ‰, which are typical
355 of mantle composition (Barrat et al., 2003).

356 Another possible explanation of the specific features of Hayyabley and Manda Hararo
357 basalts is that they might result from the interaction between ascending depleted (N-MORB
358 type) melts and the African subcontinental lithospheric mantle. Once again, such a mantle is
359 expected to be LREE-enriched (Hart et al., 1989; Vidal et al., 1991; Deniel et al., 1994) and
360 thus should transmit its trace element and isotopic fingerprint to LREE-poor ascending
361 magmas. In addition, the remarkably similar chemical features of Hayyabley, Manda Hararo
362 and E88 basalts suggest that they derive from almost identical sources and petrogenetic
363 processes. Their distinct locations, emplacement ages (Oligocene for E88, ca. 1 Ma for
364 Hayyabley and less than 0.2 Ma for Manda Hararo) and underlying crustal/lithospheric
365 thickness (normal for E88, thinned for the two other occurrences) are hardly consistent with a
366 similar petrogenetic history.

367 Therefore, as previously pointed out for the Manda Hararo basalts (Barrat et al., 2003),
368 the positive Sr, Ba and Eu anomalies and the particular Sr-Nd-Pb isotopic features of the
369 Hayyabley basalts, are more likely a genuine feature inherited from their deep mantle sources.
370 The same conclusions have been reached for depleted basalts with similar positive anomalies
371 from Iceland. Chauvel and Hémond (2000), Skovgaard et al. (2001), and Kokfelt et al. (2006)
372 have suggested that the sources of Icelandic lavas contained an old recycled oceanic

373 lithosphere component and that melting of the gabbroic portion of this lithosphere led to the
374 formation of basalts that exhibit large positive Ba, Sr and Eu anomalies. At first glance, such
375 an explanation is attractive because if this recycled gabbroic component has been
376 hydrothermally altered, one may expect $^{87}\text{Sr}/^{86}\text{Sr}$ ratios much more radiogenic than those of
377 typical MORB. Hence, the involvement of such component could account for the relatively
378 high $^{87}\text{Sr}/^{86}\text{Sr}$ ratios of the Manda Hararo and Hayyabley depleted basalts. However, an old
379 LREE-depleted recycled gabbroic component from the oceanic lithosphere would also be
380 characterized by high ϵ_{Nd} values. On the contrary, the Manda Hararo and Hayyabley lavas
381 display ϵ_{Nd} values unexpectedly low ($\epsilon_{\text{Nd}} = 5-7$) for depleted basalts. Thus, we conclude that,
382 at best, this model only partially fits the observations.

383

384 *5.2. The depleted components in the sources of Djibouti and Ethiopian basalts*

385

386 Previous geochemical studies have demonstrated the participation of a depleted
387 component during the genesis of the Horn of Africa basalts. In the case of basalts emitted by
388 the young oceanic ridges from the Red Sea or the Aden Gulf, major involvement of MORB-
389 related sources has been proposed (e.g., Barrat et al., 1990, 1993; Schilling et al., 1992;
390 Volker et al., 1993). These submarine basalts do not have the unradiogenic Pb isotopes of the
391 Carslberg Ridge ca. 1600 km east of Hayyabley volcano (Hart, 1984) but do extend away
392 from the Indian Ocean MORB toward a more HIMU composition. On land, huge volumes of
393 enriched basalts were emplaced in Afar and Ethiopia. The trace element and isotopic features
394 of the depleted reservoirs which have been involved during the genesis of the scarce LREE-
395 depleted lavas are very difficult to constrain. Two distinct LREE-depleted components have
396 been unambiguously detected.

397 First, a depleted MORB mantle component is clearly involved in the genesis of
398 Quaternary basalts from Northern Afar. The Sr-Nd-Pb isotopic relationships displayed by the
399 Erta'Ale basalts (Figs. 4 to 6) point to the participation of two mantle end-members, namely a
400 HIMU component and a depleted mantle (DM) component undistinguishable from the source
401 of the Red Sea MORB (Barrat et al., 1998). Furthermore, a similar depleted component has
402 been detected in the sources of the Oligocene lavas from the Northwestern Ethiopian volcanic
403 province (Meshesha and Shinjo, 2007). The entrainment of depleted asthenospheric mantle
404 during plume ascent (Furman et al., 2006) is a possible explanation for the contribution of this
405 component to the sources of some of the basalts erupted in Afar and Ethiopia, as well as to
406 those of Kerguelen basalts (Doucet et al., 2002). However, numerical models (Farnetani et al.,

407 2002; Farnetani and Samuel, 2005) suggest that incorporation of depleted upper mantle within
408 ascending plumes is unlikely to occur.

409 In addition, the compositions of LREE-depleted basalts from Hayyabley and Manda
410 Hararo point to a depleted end-member chemically (Fig. 3) and isotopically (Figs. 4 to 6)
411 distinct from an asthenospheric MORB-like component. A single Oligocene LREE-depleted
412 basalt displaying chemical features similar to those of the Quaternary depleted ones has been
413 collected in Ethiopia (sample E88, Pik et al., 1999). Although its isotopic composition is
414 slightly different from those of the Hayyabley basalts (Figs. 4 to 6), the occurrence of this
415 sample indicates that a depleted component distinct from the MORB source was involved in
416 this area at an early stage of plume emplacement. Therefore, we suggest that a depleted
417 component, intrinsic to the plume at depth, has contributed to the sources of both young and
418 old lavas related to the Afar plume. Similar conclusions have been reached for the Hawaiian
419 (Frey et al., 2005) and Icelandic (Thirlwall, 1995; Kerr et al., 1995; Fitton et al., 1997;
420 Chauvel and Hémond, 2000; Thirlwall et al., 2004; Skovgaard et al., 2001; Kokfelt et al.,
421 2006) plumes. However, the nature of this component is currently difficult to constrain in the
422 Afar case. Indeed, melting of the gabbroic part of an old recycled oceanic lithosphere (e.g.,
423 Kokfelt et al., 2006) would produce high ϵ_{Nd} magmas and therefore this process does not
424 account for the low ϵ_{Nd} values of Hayyableh and Manda Hararo basalts. Alternatively, LREE
425 depletion could be due to a previous melting event affecting the plume materials, as proposed
426 by Thirlwall et al. (2004) for their ID2 (or RRD2) depleted component of the Icelandic plume.
427 This hypothesis may account for the Pb isotopic differences between Hayyabley/Manda
428 Hararo basalts and the other (enriched) Djibouti basalts (Figs. 4 to 6) but can hardly explain
429 the higher Sr isotopic ratios of Hayyabley and Manda Hararo basalts.

430 Finally, another intriguing problem is the causal mechanism for the sporadic eruption of
431 small volumes of such nearly pure “depleted” melts in spatially and temporally distinct
432 locations, without any significant contamination by the dominant enriched materials. Indeed,
433 such features are difficult to reconcile with models postulating a large concentrically-zoned
434 Afar plume (e.g., Beccaluva et al., 2009). Numerical simulations of the evolution of thermal
435 and thermo-chemical plumes (Farnetani et al., 2002; Farnetani and Samuel, 2005; Farnetani
436 and Hofmann, 2009) suggest that small heterogeneous mantle domains present in the thermal
437 boundary layer feeding the plume are converted, during the ascent of the latter, into long-lived
438 elongated and narrow filaments within the plume conduit. Such filaments would melt
439 sporadically, and then eventually communicate their specific geochemical fingerprint to small
440 volumes of basaltic lavas (Farnetani and Hoffmann, 2009).

441

442 **6. Conclusions**

443

444 The ~1 Ma-old Hayyabley volcano (SE Djibouti) has emitted ca. 0.6-0.8 km³ of
445 LREE-depleted basalts ($La_n/Sm_n=0.76-0.83$) that display unusual chemical features (positive
446 Ba, Sr and Eu anomalies). These lavas are chemically distinct from the N-MORBs erupted
447 from the nearby Red Sea and Gulf of Aden oceanic ridges, and instead closely resemble the
448 LREE-depleted basalts from the Manda Hararo rift in Central Afar (Barrat et al., 2003).
449 Another similar occurrence, Oligocene in age, has been reported from the trap series in the
450 Ethiopian Plateau by Pik et al. (1999). Our new results confirm the presence within the Afar
451 region of basalts derived from an uncommon depleted component, isotopically distinct from
452 the source of the Red Sea MORBs and from the similarly depleted mantle (DM in Figs. 4 to
453 6) which contributes to the genesis of Erta' Ale volcanics (Barrat et al., 1998). This component
454 is not unusual from an isotopic (Sr, Nd, Pb, O) point of view, and is mainly recognizable from
455 the specific trace element signature of the corresponding basalts (positive Ba, Sr, Eu
456 anomalies combined with LREE depletion).

457 The origin of the Hayyabley-Manda Hararo basalts fingerprint could be ascribed to the
458 interactions between (i) depleted (N-MORB type) basalts derived from an asthenospheric
459 mantle component similar to the Erta 'Ale depleted end-member and (ii) enriched lithospheric
460 materials which would be responsible for the positive Ba, Sr and Eu anomalies. These
461 materials could be either the African continental crust, flood basalt-related gabbroic
462 cumulates stored within or below it, or finally the subcontinental lithospheric mantle.
463 However, all these materials are mostly LREE-enriched, and the contamination hypothesis can
464 hardly explain the clear LREE, Rb and Th depletion and concomitant Ba, Sr and Eu
465 enrichment of Hayyabley basalts (Figs. 2 and 3) as well as their Pb isotopic signature (Figs. 5
466 and 6). Moreover, contamination in plume-related volcanic series is often described as a
467 variable, occasional or random process. Thus, it can hardly account for the very specific trace
468 element and isotopic signature of the Afar depleted basalts, which were erupted in three
469 separate locations, with distinct emplacement ages and underlying crustal/lithospheric
470 thickness.

471 Therefore, our preferred conclusion is that these depleted basalts derive from a intrinsic
472 (although volumetrically minor) depleted component from the Afar plume, possibly present as
473 elongated and narrow filaments within the plume conduit. Sporadic melting of such filaments

474 might account for the restricted spatial and temporal distribution of the Afar depleted basalts.
475 The precise origin of this deep mantle component is currently difficult to constrain, given the
476 small number of depleted basalt samples and the limited amount of corresponding
477 geochemical data. The most likely hypothesis is the contribution of recycled gabbros from
478 ancient oceanic crust.

479

480 **Acknowledgements**

481

482 This study has been funded by the French Embassy in Djibouti, and the grant of the first author (M.A.D.)
483 provided by the MAWARI international program managed by the CIFEG, Orléans, France. Analytical expenses
484 were funded by the MAWARI program and UMR 6538, Plouzané. We especially thank Dr. Mohamed Jalludin,
485 Director of the CERD, for his interest, scientific discussions and logistic support, Ali Abdillahi for his efficiency
486 in organizing fieldwork, and Marcel Bohn for his help with microprobe analysis. Careful reviews by Tania
487 Furman and Godfrey Fitton led us to improve significantly the organization and contents of this manuscript.

488

489 **References**

490

491 Baker, J.A., Thirlwall, M.F., Menzies, M.A., 1996. Sr-Nd-Pb isotopic and trace element
492 evidence for crustal contamination of plume-derived flood basalts: Oligocene flood
493 volcanism in Western Yemen. *Geochimica et Cosmochimica Acta* 60, 2559-2581.

494

495 Barberi, F., Ferrara, G., Santacroce, R., Varet, J., 1975. Structural evolution of the Afar
496 triple junction. In: Pilger, A., Rösler, A., (Eds.) *Afar Depression of Ethiopia*.
497 Schweizerbart, Stuttgart, 38-54.

498

499 Barberi, F., Varet, J., 1977. Volcanism in Afar, small scale plate tectonics implications.
500 *Geological Society of America Bulletin* 88, 1251-1266.

501

502 Barrat, J.A., Keller, F., Amossé, J., Taylor, R.N., Nesbitt, R.W., Hirata, T., 1996.
503 Determination of rare earth elements in sixteen silicate reference samples by ICP-MS
504 after Tm addition and ion exchange separation. *Geostandards Newsletter* 20, 133-139.

505

506 Barrat, J.A., Fourcade, S., Jahn, B.M., Cheminée, J.L., Capdevila, R., 1998. Isotope (Sr, Nd,
507 Pb, O) and trace-element geochemistry of volcanics from the Erta'Ale range (Ethiopia).
508 *Journal of Volcanology and Geothermal Research* 80, 85-100.

509

510 Barrat, J.A., Jahn, B.M., Joron, J.L., Auvray, B., Hamdi, H., 1990. Mantle heterogeneity in
511 northeastern Africa: evidence from Nd isotopic compositions and hygromagmaphile
512 element geochemistry of basaltic rocks from the Gulf of Tadjoura and Southern Red Sea
513 regions. *Earth and Planetary Science Letters* 101, 233-247.

514

515 Barrat, J.A., Jahn, B.M., Fourcade, S., Joron, J.L., 1993. Magma genesis in an ongoing
516 rifting zone: the Tadjoura Gulf. *Geochimica et Cosmochimica Acta* 57, 2291-2302.

517

518 Barrat, J.A., Blichert-Toft, J., Gillet, P., Keller, F., 2000. The differentiation of eucrites: the
519 role of *in situ* crystallization. *Meteoritics & Planetary Science* 35, 1087-1100.

520

521 Barrat, J.A., Joron, J.L., Taylor, R.N., Fourcade, S., Nesbitt, R.W., Jahn, B.M., 2003.
522 Geochemistry of basalts from Manda Hararo, Ethiopia: LREE-depleted basalts in
523 Central Afar. *Lithos* 69, p. 1-13.

524

525 Barrat, J.A., Yamaguchi, A., Greenwood, A., Bohn, M., Cotten, J., Benoit, M., Franchi,
526 I.A., 2007. The Stannern trend eucrites: contamination of main group eucritic magmas
527 by crustal partial melts. *Geochimica et Cosmochimica Acta* 71, 4108-4124.

528

529 Beccaluva, L., Bianchini, G., Natali, C., Siena, F., 2009. Continental flood basalts and
530 mantle plumes: a case study of the Northern Ethiopian Plateau. *Journal of Petrology*
531 50, 1377-1403.

532

533 Blichert-Toft, J., White, W.M., 2001. Hf isotope geochemistry of the Galapagos Islands.
534 *Geochemistry, Geophysics, Geosystems* 2, doi:10.129/2000GC000138.

535

536 Charbit, S., Guillou, H., Turpin, L., 1998. Cross calibration of K-Ar standard minerals using
537 an unspiked Ar measurement technique. *Chemical Geology* 150, 147-159.

538

539 Chauvel, C., Hémond C., 2000. Melting of a complete section of recycled oceanic crust:
540 trace element and Pb isotopic evidence from Iceland. *Geochemistry, Geophysics,*
541 *Geosystems* 1, paper number 1999GC000002.

542

543 Chen, C.-Y., Frey, F.A., 1985. Trace element and isotope geochemistry of lavas from
544 Halaakala Volcano, East Maui: implications for the origin of Hawaiian basalts. *Journal*
545 *of Geophysical Research* 90, 8743-8768.

546

547 Cotten, J., Le Dez, A., Bau, M., Caroff, M., Maury, R.C., Dulski, P., Fourcade, S., Bohn,
548 M., Brousse, R., 1995. Origin of anomalous rare-earth element and yttrium
549 enrichments in subaerially exposed basalts: Evidence from French Polynesia.
550 *Chemical Geology* 119, 115-138.

551

552 Courtillot, V., Galdeano, A., Le Mouel, J.-L., 1980. Propagation of an accreting plate
553 boundary: a discussion of new magnetic data in the Gulf of Tadjoura and Southern Afar.
554 *Earth and Planetary Science Letters* 47, 144-160.

555

556 Courtillot, V., Achache, J., Landre, F., Bonhommet, N., Montigny, R., Féraud, G., 1984.
557 Episodic spreading and rift propagation: new paleomagnetic and geochronologic data
558 from the Afar nascent passive margin. *Journal of Geophysical Research* 89, 3315-3333.

559

560 Daoud, M.A., 2008. Dynamique du rifting continental de 30 Ma à l'Actuel dans la partie
561 sud-est du Triangle Afar. Tectonique et magmatisme du rift de Tadjoura et des
562 domaines Danakil et d'Ali Sabieh, République de Djibouti. Thèse, Université de
563 Bretagne Occidentale, Brest, 190 p.

564

565 Defant, M.J., Maury, R.C., Ripley, E.M., Feigenson, M.D., Jacques, D., 1991. An example
566 of island-arc petrogenesis: geochemistry and petrology of the southern Luzon arc,
567 Philippines. *Journal of Petrology* 32, 455-500.

568

569 Deniel, C., Vidal, P., Coulon, C., Vellutini, P.J., Piguet, P., 1994. Temporal evolution of
570 mantle sources during continental rifting: the volcanism of Djibouti (Afar). *Journal of*
571 *Geophysical Research* 99, 2853-2869.

572

573 Dosso, L., Bougault, H., Joron, J.L., 1993. Geochemical morphology of the North Mid-
574 Atlantic Ridge, 10°-24°N: trace element-isotope complementary. *Earth and Planetary*
575 *Science Letters* 120, 443-462.

576
577
578
579
580
581
582
583
584
585
586
587
588
589
590
591
592
593
594
595
596
597
598
599
600
601
602
603
604
605
606

Doucet, S., Weis, D., Scoates, J.S., Nicolaysen, K., Frey, F.A., Giret, A., 2002. The depleted mantle component in Kerguelen Archipelago basalts: petrogenesis of tholeiitic-transitional basalts from the Loranchet Peninsula. *Journal of Petrology* 43, 1341-1366.

Dugda, M.T., Nyblade, A.A., 2006. New constraints on crustal structure in eastern Afar from the analysis of receiver functions and surface wave dispersion in Djibouti. In: Yirgu, G., Ebinger, C.J., Maguire, P.K.H., (Eds.), *The Afar volcanic province within the East African Rift System*. Geological Society of London, Special Publication 259, 239-251.

Evensen, N.M., Hamilton, P.J., O'Nions, R.K., 1978. Rare Earth abundances in chondritic meteorites. *Geochimica et Cosmochimica Acta* 42, 1199-1212.

Farnetani, C.G., Legras, B., Tackley, P.J., 2002. Mixing and deformation in mantle plumes. *Earth and Planetary Science Letters*, 196, 1-15.

Farnetani, C.G., Samuel, H., 2005. Beyond the thermal plume paradigm. *Geophysical Research Letters*, 32, L07311, doi:10.129/2005GL022360.

Farnetani, C.G., Hofmann, A.W., 2009. Dynamics and internal structure of a lower mantle plume conduit. *Earth and Planetary Science Letters*, 282, 314-322.

Fitton, J.G., Saunders, A.D., Norry, M.J., Hardason, B.S., Taylor, R.N., 1997. Thermal and chemical structure of the Iceland plume. *Earth and Planetary Science Letters*, 153, 197-208.

Fitton, J.G., Saunders, A.D., Kempton, P.D., Hardason, B.S., 2003. Does depleted mantle form an intrinsic part of the Iceland plume? *Geochemistry, Geophysics, Geosystems* 4, 2002GC000424.

607 Fournier, M., Gasse, F., Lépine, J.-C., Richard O., Ruegg J.C., 1982. Carte géologique de la
608 République de Djibouti à 1:100 000. Djibouti. ISERST. Ministère français de
609 Coopération. Ed. ORSTOM, Paris.

610

611 Frey, F.A., Huang, S., Blichert-Toft, J., Regelous, M., Boyet, M., 2005. Origin of depleted
612 components in basalt related to the Hawaiian hot spot: Evidence from isotopic and
613 incompatible element ratios. *Geochemistry, Geophysics, Geosystems* 6, Q02L07,
614 doi:10.129/2004GC000757.

615

616 Fuhrmann, U., Lippolt, H., Hess, J.C., 1987. HD-B1 Biotite reference material for K-Ar
617 chronometry. *Chemical Geology* 66, 41-51.

618

619 Furman, T., Bryce, J., Rooney, T., Hana, B., Yirgu, G., Ayalew, D., 2006. Heads and tails:
620 30 million years of the Afar plume. In: Yirgu, G., Ebinger, C.J., Maguire, P.K.H.,
621 (Eds.), *The Afar volcanic province within the East African Rift System*. Geological
622 Society of London, Special Publication 259, 95-119.

623

624 Gasse, F., Fournier, M., Richard, O., Ruegg, J.C., 1983. Carte géologique de la République
625 de Djibouti à 1:100 000. Djibouti. Notice explicative. ISERST, Ministère français de la
626 Coopération, Ed. ORSTOM, Paris, 70 pp.

627

628 Guillou, H., Singer, B., Laj, C., Kissel, C., Scaillet, S., Jicha, B.R., 2004. On the age of the
629 Laschamp geomagnetic event. *Earth and Planetary Science Letters*, 227, 331-343.

630

631 Hart, S.R., 1984. A large-scale isotope anomaly in the Southern Hemisphere mantle. *Nature*
632 309, 753-757.

633

634 Hart, S.R., 1988. Heterogeneous mantle domains: signatures, genesis and mixing
635 chronologies. *Earth and Planetary Science Letters* 90, 273-296.

636

637 Hart, S.R., Hauri, E.H., Oschmann, L.A., Whitehead, J.A., 1992. Mantle plumes and
638 entrainment: isotopic evidence. *Science* 256, 517-520.

639

640 Hart, W.K., Woldegabriel, G., Walter, R.C., Mertzman, S.A., 1989. Basaltic volcanism in
641 Ethiopia: constraints on continental rifting and mantle interactions. *Journal of*
642 *Geophysical Research* 94, 7731-7748.

643

644 Hase, K.M., Mühe, R., Stoffers, P., 2000. Magmatism during extension of the lithosphere:
645 geochemical constraints from lavas of the Shaban Deep, northern Red Sea. *Chemical*
646 *Geology* 166, 225-239.

647

648 Hémond, C., Arndt, N.T., Lichtenstein, U., Hofmann, A., 1993. The heterogeneous Iceland
649 plume: Nd-Sr-O isotopes and trace element constraints. *Journal of Geophysical*
650 *Research* 98, 15803-15850.

651

652 Hoernle, K., Werner, R., Phipps-Morgan, J., Garbe-Schönberg, D., Bryce, J., Mrazek, J.,
653 2000. Existence of complex spatial zonation in the Galapagos plume for at least 14 m. y.
654 *Geology* 28, 435-438.

655

656 Ishizuka, O., Taylor, R.N., Milton, J.A., Nesbitt, R.W., 2003. Fluid-mantle interaction in an
657 intraoceanic arc: constraints from high-precision Pb isotopes. *Earth and Planetary*
658 *Science Letters* 211, 221-236.

659

660 Ito, E., White, W.M., Göpel, C., 1987. The O, Sr, Nd, and Pb isotope geochemistry of
661 MORB. *Chemical Geology* 62, 157-176.

662

663 Joron, J.L., Treuil, M., Jaffrezic, H., Villemant, B., Richard, O., 1980. Géochimie des
664 éléments en traces du volcanisme de l'Afar et de la mégastructure Mer Rouge-Afar-
665 Golfe d'Aden. Implications pétrogénétiques et géodynamiques. *Bulletin de la Société*
666 *géologique de France* (7) 22, 945-957.

667

668 Johnson, C.M., Beard, B.L., 1999. Correction of instrumentally produced mass
669 fractionation during isotopic analysis of Fe by thermal ionization mass spectrometry,
670 *International Journal of Mass Spectrometry* 193, 87-99.

671

672 Kerr, A.C., Saunders, A.D., Tarney, J., Berry, N.H., Hards, V.L., 1995. Depleted mantle-
673 plume geochemical signatures: No paradox for plume theories. *Geology* 23, 843-846.

674
675
676
677
678
679
680
681
682
683
684
685
686
687
688
689
690
691
692
693
694
695
696
697
698
699
700
701
702
703
704
705
706

Kokfelt, T.F., Hoernle, K., Hauf, F., Fiebig, J., Werner, R., Garbe-Schomberg, D., 2006. Combined trace element and Pb-Nd-Sr-O isotope evidence for recycled oceanic crust(upper and lower) in the Iceland mantle plume. *Journal of Petrology* 47, 1705-1749.

Laughlin, A.W., Poths, S., Healey, H., Reneau, S., Woldegabriel, G., 1994. Dating Quaternary basalts using the ^3He and ^{14}C methods with implications for excess Ar. *Geology* 22, 135-138.

Lin, S.-S., Keken, P.E. van, 2006. Dynamics of thermochemical plumes: 2. Complexity of plume structures and its implications for mapping mantle plumes. *Geochemistry, Geophysics, Geosystems* 7, Q033003, doi:10.129/2005GC001072.

Manighetti, I., Tapponnier, P., Courtillot, V., Gruszow, S., Gillot., P.Y., 1997. Propagation of rifting along the Arabia-Somalia plate boundary: the Gulfs of Aden and Tadjoura. *Journal of Geophysical Research* 102, 2681-2710.

Meshesha, D., Shinjo, R., 2007. Crustal contamination and diversity of magma sources in the Northwestern Ethiopian volcanic province. *Journal of Mineralogical and Petrological Sciences*, 102, 272-290.

Needham, H.D., Choukroune, P., Cheminée, J.-L., Le Pichon, X., Francheteau, J., Tapponnier, P., 1976. The accreting plate boundary: Ardoukobâ Rift (N.E. Africa) and the oceanic Rift valley. *Earth and Planetary Science Letters* 28, 439-453.

Odin, G.S., and 35 collaborators, 1982. Interlaboratory standards for dating purposes. In: Odin G.S., (Ed.), *Numerical dating in stratigraphy*, Wiley, Chichester, 123-149.

Pik, R., Deniel, C., Coulon, C., Yirgu, G., Hoffmann, C., Ayalew, D., 1998. The northwestern Ethiopian Plateau flood basalts: Classification and spatial distribution of magma types. *Journal of Volcanology and Geothermal Research* 81, 91-111.

707 Pik, R., Deniel, C., Coulon, C., Yirgu, G., Marty, B., 1999. Isotopic and trace element
708 signatures of Ethiopian flood basalts: evidence for plume-lithosphere interactions.
709 *Geochimica et Cosmochimica Acta* 63, 2263-2279.
710

711 Richard, O. 1979. Etude de la transition dorsale océanique – rift émergé: le golfe de
712 Tadjoura (République de Djibouti). Approche géologique, géochronologique et
713 pétrologique. Thèse 3^{ème} cycle, Université de Paris XI-Orsay, 149 p.
714

715 Rogers, N.W., 2006. Basaltic magmatism and the geodynamics of the East African Rift
716 System. In: Yirgu, G., Ebinger, C.J., Maguire, P.K.H., (Eds.), *The Afar volcanic
717 province within the East African Rift System*. Geological Society of London, Special
718 Publication 259, 77-93.
719

720 Saal, A.E., Kurtz, M.D., Hart, S.R., Blusztajn, J.S., Blichert-Toft, J., Liang, Y., Geist, D.J.,
721 2007. The role of lithospheric gabbros on the composition of Galapagos lavas. *Earth
722 and Planetary Science Letters* 257, 391-406.
723

724 Scaillet, S., Guillou, H., 2004. A critical evaluation of young (near-zero) K-Ar ages. *Earth
725 and Planetary Science Letters* 220, 265-275.
726

727 Schilling, J.G., 1973. Afar mantle plume: rare earth evidence. *Nature* 242, 2-5.
728

729 Schilling, J.G., Kingsley, R.H., Hanan, B.B., McCully, B.L., 1992. Nd-Sr-Pb variations
730 along the Gulf of Aden: evidence for Afar Mantle plume-continental lithosphere
731 interaction. *Journal of Geophysical Research* 97, 10927-10966.
732

733 Skovgaard, A.C., Storey, M., Baker, J., Blusztajn, J., Hart, S.R., 2001. Osmium-oxygen
734 isotopic evidence for a recycled and strongly depleted component in the Iceland mantle
735 plume. *Earth and Planetary Science Letters* 194, 259-275.
736

737 Steiger, R.H., Jäger, E., 1977. Subcommittee on geochronology: convention on the use of
738 decay constants in geo- and cosmochemistry. *Earth and Planetary Science Letters* 36,
739 359-362.
740

741 Stieltjes, L., Joron, J.L., Treuil, M., Varet, J., 1976. Le rift d'Asal, segment de dorsale
742 émergée: discussion pétrologique et géochimique. Bulletin de la Société géologique de
743 France (7) 18, 851-862.
744

745 Sun, S.S., McDonough, W.F., 1989. Chemical and isotopic systematics of oceanic basalts:
746 Implications for mantle composition and processes. In: Saunders, A.D., Norry, M.J.,
747 (Eds.), Magmatism in the ocean basins. Geological Society of London Special
748 Publication 42, 313-345.
749

750 Taylor, R.N., Thirlwall, M.F., Murton, B.J., Hilton, D.R., Gee, M.A.M., 1997. Isotopic
751 constraints on the influence of the Icelandic plume. Earth and Planetary Science Letters
752 148, 1-8.
753

754 Thirlwall, M.F., 1995. Generation of the Pb isotopic characteristics of the Iceland plume.
755 Journal of the Geological Society of London, 152, 991-996.
756

757 Thirlwall, M.F., Gee, M.A.M., Taylor, R.N., Murton, B.J., 2004. Mantle components in
758 Iceland and adjacent ridges investigated using double-spike Pb isotope ratios.
759 Geochimica et Cosmochimica Acta 68, 361-386.
760
761

762 Treuil, M., Joron, J.L., 1975. Utilisation des éléments hygromagmatophiles pour la
763 simplification de la modélisation quantitative des processus magmatiques. Exemples de
764 l'Afar et de la dorsale médioatlantique. Rendiconti della Società Italiana di Mineralogia
765 e Petrologia 31, 125-174.
766

767 Vidal, P., Deniel, C., Vellutini, P.J., Piguet, P., Coulon, C., Vincent, J., Audin, J., 1991.
768 Changes of mantle sources in the course of a rift evolution: the Afar case. Geophysical
769 Research Letters 18, 1913-1916.
770

771 Volker, F., Altherr, R., Jochum, K.P., McCulloch, M.T., 1997. Quaternary volcanic activity
772 of the southern Red Sea: new data and assessment of models on magma sources and
773 Afar plume-lithosphere interaction. Tectonophysics 278, 15-29.
774

- 775 Volker, F., McCulloch, M.T., Altherr, R., 1993. Submarine basalts from the Red Sea: new
776 Pb, Sr, and Nd isotopic data. *Geophysical Research Letters* 20, 927-930.
777
- 778 White, W.M., McBirney, A.R., Duncan, R.A., 1993. Petrology and geochemistry of the
779 Galapagos islands: portrait of a pathological mantle plume. *Journal of Geophysical*
780 *Research* 98, 19533-19563.
781
- 782 Yang, H.-J., Frey, F.A., Clague, D.A., 2003. Constraints on the source components of lavas
783 forming the Hawaiian North Arch and Honolulu volcanoes. *Journal of Petrology* 44,
784 603-627.
785
- 786 Yurtmen, S., Guillou, H., Orhan, O., Rowbotham, G., Westaway, R., 2002. Rate of strike-
787 slip on the Amanos Fault (Karasu Valley, southern Turkey) constrained by K-Ar dating
788 and geochemical analysis of Quaternary basalts. *Tectonophysics* 344, 207-246.
789
- 790 Zindler, A., Hart, S.R., Frey, F.A., Jakobsson, S.P., 1979. Nd and Sr isotope ratios and rare
791 earth abundances in Reykjanes Peninsula basalts: evidence for mantle heterogeneity
792 beneath Iceland. *Earth and Planetary Science Letters* 45, 249-262.
793
- 794 Zumbo, V., Féraud, G., Vellutini, H., Pigué, P., Vincent, J., 1995. First $^{40}\text{Ar}/^{39}\text{Ar}$ dating on
795 Early Pliocene to Plio-Pleistocene magmatic events of the Afar – Republic of Djibouti.
796 *Journal of Volcanology and Geothermal Research* 65, 281-295.
797

798 **Figure captions**

799
800 Fig. 1. Geological setting of the Djibouti Plain. (a) Location of the study area in the Tadjoura
801 Gulf context. (b) ASTER satellite image showing the Hayyabley volcano post-dating the
802 coastal fault belt related to the Tadjoura rift. (c) Geological interpretation of Fig. 1b.
803

804 Fig. 2. Chondrite-normalized REE patterns of Hayyableh basalts compared to the field of
805 older Tadjoura Gulf basalts located onland in Djibouti (Barrat et al., 1993; Daoud, 2008). The
806 reference chondrite is from Evensen et al. (1978). The pattern of a southern Red Sea N-
807 MORB (sample V84, Barrat et al., 1990) is shown for comparison.
808

809 Fig. 3. Primitive mantle-normalized element patterns for Hayyabley basalts, LREE-depleted
810 Manda Hararo basalts (Barrat et al., 2003), two submarine MORB from the East of the Gulf
811 of Tadjoura (Barrat et al., 1990, 1993), the southern Red Sea N-MORB sample V84 (Barrat
812 et al., 1990), and the LREE-depleted sample E88 from the Oligocene Ethiopian Plateau (Pik
813 et al., 1999). The primitive mantle values are from Sun and McDonough (1989).

814

815 Fig. 4. Plot of ϵ_{Nd} vs. $^{87}Sr/^{86}Sr$ for young onland basalts from Djibouti (Deniel et al., 1994, and
816 this study). Only the two reliable Sr isotopic ratios of Hayyabley basalts have been plotted.
817 Basalts older than 4 Ma have been omitted because of their possible contamination by
818 continental crust. The fields of (1) basalts from the South Red Sea occurrences, which include
819 oceanic ridge segments, Ramad seamount and Zubair and Hanish islands (Barrat et al., 1990,
820 1993; Volker et al., 1993, 1997), (2) submarine basalts from the East of the Gulf of Tadjoura
821 and the Aden Gulf (Barrat et al., 1990, 1993; Schilling et al., 1992), (3) Erta 'Ale volcanics
822 (Barrat et al., 1998), (4) LREE-depleted basalts from Manda Hararo (MH, Barrat et al., 2003),
823 and (5) some Ethiopian samples (E88: depleted Oligocene basalt; HT2: average composition
824 of high-Ti basalts, Pik et al., 1999) are shown for comparison. DM refers to the regional
825 depleted mantle composition deduced from the study of South Red Sea and Gulf of Aden
826 basalts.

827

828 Fig. 5. Plot of $^{207}Pb/^{204}Pb$ and $^{208}Pb/^{204}Pb$ vs. $^{206}Pb/^{204}Pb$ for young (less than 4 Ma) onland
829 enriched basalts from Djibouti (Deniel et al., 1994) and Hayyabley depleted basalts (this
830 study). Other fields as in Fig. 4. E'A: field of Erta 'Ale volcanics (Barrat et al., 1998). Most
831 $^{207}Pb/^{204}Pb$ data taken from the regional literature (e.g. on E88 and Erta 'Ale) are less precise
832 than those measured on Hayyabley basalts, and should therefore be considered with caution.

833

834 Fig. 6. Plot of $^{206}Pb/^{204}Pb$ vs. ϵ_{Nd} for young (less than 4 Ma) onland enriched basalts from
835 Djibouti (Deniel et al., 1994) and Hayyabley depleted basalts (this study). Other fields as in
836 Fig. 5.

837

838 **Table captions**

839

840 Table 1. Unspiked ^{40}K - ^{40}Ar datings of Hayyabley basalts. See text for the analytical
841 procedures.

842

843 Table 2. Major and trace element analyses of Hayyabley basalts (major oxides in wt%, trace
844 elements in ppm). ICP-AES and ICP-MS analytical methods described in the text.

845

846 Table 3. Compositions of LREE-depleted basalts from Hayyabley (average of the samples
847 analysed by ICP-MS), Manda Hararo (average data from Barrat et al., 2003), Ethiopian
848 Plateau (sample E88, Pik et al., 1999), and of a N-MORB from Tadjoura Gulf (sample A3D3,
849 Joron et al., 1980; Barrat et al., 1993). Major oxides in wt%, trace elements in ppm. n denotes
850 ratios normalized to the primitive mantle composition from Sun and McDonough (1989).

851

852 Table 4. Sr, Nd and Pb isotopic compositions of Hayyabley basalts (B: bulk rock; R: residue
853 after leaching). See text for the analytical procedures. $\Delta 7/4$ and $\Delta 8/4$ denote the deviation (in
854 ‰) of $^{207}\text{Pb}/^{204}\text{Pb}$ and $^{208}\text{Pb}/^{204}\text{Pb}$ ratios with respect to the Northern Hemisphere Reference
855 Line (NHRL: Hart, 1984, 1988).

1 A LREE-depleted component in the Afar plume: further 2 evidence from Quaternary Djibouti basalts

3
4

5 Mohamed A. Daoud ^{a,b}, René C. Maury ^{a*}, Jean-Alix Barrat ^a, Rex N.
6 Taylor ^c, Bernard Le Gall ^a, Hervé Guillou ^d, Joseph Cotten ^a, Joël Rolet ^a

7
8

9 ^a *Université Européenne de Bretagne, Université de Brest; CNRS; UMR 6538 Domaines Océaniques;*
10 *Institut Universitaire Européen de la Mer, Place N. Copernic, 29280 Plouzané, France.*

11 ^b *Centre d'Etudes et de Recherches Scientifiques de Djibouti, B.P. 486, Djibouti.*

12 ^c *School of Ocean and Earth Science, NOC, University of Southampton, Southampton SO14 3ZH, UK.*

13 ^d *UMR 1572 LSCE/CEA-CNRS, Domaine du CNRS, 12 avenue de la Terrasse, 91118 Gif-sur-Yvette,*
14 *France.*

15
16

* Corresponding author. Tel.: (33)298498708; fax: (33)298498760

17 *E-mail address: maury@univ-brest.fr*

18
19

Abstract

20
21

Major, trace element and isotopic (Sr, Nd, Pb) data and unspiked K-Ar ages are presented for Quaternary
22 (0.90-0.95 Ma old) basalts from the Hayyabley volcano, Djibouti. These basalts are LREE-depleted ($La_n/Sm_n =$
23 $0.76-0.83$), with $^{87}Sr/^{86}Sr$ ratios ranging from 0.70369 to 0.70376, and rather homogeneous $^{143}Nd/^{144}Nd$ ($\epsilon_{Nd} =$
24 $+5.9 - +7.3$) and Pb isotopic compositions ($^{206}Pb/^{204}Pb = 18.47-18.55$, $^{207}Pb/^{204}Pb = 15.52-15.57$, $^{208}Pb/^{204}Pb =$
25 $38.62-38.77$). They are very different from the underlying enriched Tadjoura Gulf basalts, and from the N-
26 MORB erupted from the nascent oceanic ridges of the Red Sea and Gulf of Aden. Their compositions closely
27 resemble those of (1) depleted Quaternary Manda Hararo basalts from the Afar depression in Ethiopia and (2)
28 one Oligocene basalt from the Ethiopian Plateau trap series. Their trace element and Sr, Nd, Pb isotope
29 systematics suggest the involvement of a discrete but minor LREE-depleted component, which is probably an
30 intrinsic part of the Afar plume.

31
32

1. Introduction.

33
34

The study of basalts from intra-oceanic islands and plateaus as well as from traps and
35 rifts has shown the considerable chemical heterogeneity of plume materials (Hart, 1988). This

36 heterogeneity might indicate very complex plume structures and dynamics (Lin and van
37 Keken, 2006). However, it may not only result from the initial chemical heterogeneity of
38 mantle plumes at depth but also from the entrainment of surrounding mantle materials (Hart et
39 al., 1992; Furman et al., 2006). In addition, a lithospheric component is clearly recognized in
40 some intracontinental basalts, e.g. in the Afar province, but its origin is still debated (Rogers,
41 2006). Some authors have suggested that melting of the Afar lithospheric mantle explains a
42 significant proportion of the erupted lavas (Hart et al., 1989; Vidal et al., 1991; Deniel et al.,
43 1994) whilst others point out that continental crust contamination [can also contribute to the](#)
44 isotopic signature of these basalts (Barrat et al., 1993; Baker et al., 1996; Pik et al., 1999).

45 [The vast majority of plume-related basalts, including the Afar ones \(Furman et al., 2006;](#)
46 [Beccaluva et al., 2009\) are dominated by a component that is chemically and isotopically](#)
47 [enriched. However, the](#) occurrence of subordinate components characterized by a light rare
48 earth element (LREE) depletion has been suggested from the study of basalts from major
49 mantle plumes in: (1) Iceland (Zindler et al., 1979; Hémond et al., 1993; Taylor et al., 1997;
50 Chauvel and Hémond, 2000; Skovgaard et al., 2001; Fitton et al., 2003; Thirlwall et al., 2004;
51 Kokfelt et al., 2006); (2) Hawaii (Chen and Frey, 1985; Yang et al., 2003; Frey et al., 2005);
52 (3) the Galapagos (White et al., 1993; Hoernle et al., 2000; Blichert-Toft and White, 2001;
53 Saal et al., 2007); and (4) the Kerguelen Archipelago (Doucet et al., 2002). However, the
54 characterization of this reservoir is difficult because its signature may be overprinted by either
55 the dominant enriched plume component or the lithospheric reservoirs. Therefore, [the](#)
56 [presence of an intrinsic depleted component in plumes is still an open question.](#)

57 LREE-depleted basalts associated to the Afar mantle plume have long been recognized
58 in the Quaternary Manda Hararo volcanic chain, Ethiopia (Treuil and Joron, 1975; Joron et
59 al., 1980; Barrat et al., 2003). A single LREE-depleted Oligocene Ethiopian Plateau basalt has
60 also been so far analysed ([sample E88](#): Pik et al., 1998, 1999). The purpose of this paper is:
61 (1) to describe another newly discovered occurrence of such basalts in the SE part of the Afar
62 triangle, i.e. the rather large Hayyabley Quaternary volcano in Djibouti (Fig. 1), and (2) to
63 discuss its bearing on the composition and heterogeneity of the Afar mantle plume.

64

65 **2. Analytical techniques**

66

67 Ar isotopic compositions and K contents (Table 1) were measured at Gif-sur-Yvette and
68 IUEM (Institut Universitaire Européen de la Mer), respectively. The samples were crushed,
69 sieved to 0.25-0.125 mm size fraction and ultrasonically washed in acetic acid. Potassium and

70 argon were measured on the microcrystalline groundmass, after removal of phenocrysts using
71 heavy liquids of appropriate densities and magnetic separations. This process improves the K
72 yield as well as the percentage of radiogenic argon, and removes at least some potential
73 sources of systematic error due to the presence of excess ^{40}Ar in olivine and feldspar
74 phenocrysts (Laughlin et al., 1994). Ar analyses were performed using the procedures detailed
75 in Yurtmen et al. (2002) and Guillou et al. (2004). The unspiked technique differs from the
76 conventional isotope dilution method in that argon extracted from the sample is measured in
77 sequence with purified aliquots of atmospheric argon at the same working gas pressure in the
78 mass-spectrometer. This suppresses mass discrimination effects between the atmospheric
79 reference and the unknown, and allows quantities of radiogenic $^{40}\text{Ar}^*$ as small as 0.14% to be
80 detected on a single-run basis (Scaillet et al., 2004). Argon was extracted by radio frequency
81 heating of 2.0 – 3.0 g of sample, then transferred to an ultra-high-vacuum glass line and
82 purified with titanium sponge and Zr-Ar getters. Isotopic analyses were performed on total
83 ^{40}Ar contents ranging between 2.4 and 3.2×10^{-11} moles using a 180°, 6 cm radius mass
84 spectrometer with an accelerating potential of 620V. The manometric calibration (Charbit et
85 al., 1998) was based on periodic, replicate determinations of international dating standards
86 including LP-6 (Odin et al., 1982) and HD-B1 (Fuhrmann et al., 1987). The total ^{40}Ar content
87 of the sample can be determined with a precision of $\pm 0.2\%$ (2σ) according to this procedure.
88 Ages were calculated using the constants recommended by Steiger and Jäger (1977).

89 Major element compositions of minerals and glasses were determined using a Cameca
90 SX50 five spectrometer automated electron microprobe (Microsonde Ouest, Plouzané,
91 France). Analytical conditions were 15 kV, 10-12 nA and a counting time of 6 sec. (see
92 Defant et al., 1991, for further analytical details). Major and trace element data on bulk rocks
93 (Table 2) were first obtained by Inductively Coupled Plasma-Atomic Emission Spectrometry
94 (ICP-AES) at IUEM, Plouzané. The samples were finely powdered in an agate grinder.
95 International standards were used for calibration tests (ACE, BEN, JB-2, PM-S and WS-E).
96 Rb was measured by flame emission spectroscopy. Relative standard deviations are $\pm 1\%$ for
97 SiO_2 , and $\pm 2\%$ for other major elements except P_2O_5 and MnO (absolute precision $\pm 0.01\%$),
98 and ca. 5% for trace elements. The analytical techniques are described in Cotten et al. (1995).
99 Concentrations of additional trace elements were measured by Inductively Coupled Plasma
100 Mass Spectrometry (ICP-MS) at IUEM, using a Thermo Element 2 spectrometer following
101 procedures adapted from Barrat et al. (1996, 2000). Based on standard measurements and
102 sample duplicates, trace element concentration reproducibility is generally better than 5 %
103 (Barrat et al., 2007), and are in good agreement with the ICP-AES results (Table 2).

104 Isotopic compositions of Sr and Nd (Table 4) were determined at IUEM. Conventional
105 ion exchange techniques were used for separation of Sr, and isotope ratio measurements were
106 carried out by thermal ionization mass spectrometry using a Thermo Triton equipped with 7
107 collectors. Isotopic ratios were normalized for instrumental mass fractionation relative to
108 $^{86}\text{Sr}/^{88}\text{Sr} = 0.1194$. $^{87}\text{Sr}/^{86}\text{Sr}$ of the NBS 987 Sr standard yielded 0.710213 ± 22 (2σ , $n=14$) and
109 the sample Sr isotopic compositions are reported relative to $^{87}\text{Sr}/^{86}\text{Sr} = 0.71024$. The Nd
110 purification was done according to the procedure described in Dosso et al. (1993). TRU Spec
111 chromatographic resins from Eichrom were used to separate the REE fraction from the sample
112 matrix. Then, the separation and elution of Nd and other REE were realized on Ln.Spec resin.
113 During the course of the study, analyses of the La Jolla standard were performed and gave an
114 average of $^{143}\text{Nd}/^{144}\text{Nd} = 0.511845 \pm 6$ ($n=15$). All Nd data were fractionation-corrected to
115 $^{146}\text{Nd}/^{144}\text{Nd} = 0.7219$ and further normalized to a value of $^{143}\text{Nd}/^{144}\text{Nd} = 0.511860$ for the La
116 Jolla standard.

117 Isotopic compositions of Pb were determined at the National Oceanography Centre,
118 Southampton, using the SBL 74 double spike. Powdered samples were leached with 6 M HCl
119 at 140°C for 1 hour and then rinsed up to 6 times with ultrapure water prior to dissolution.
120 Lead separation was then performed on an anionic exchange resin. High-resolution Pb
121 isotopic analyses were carried out on a VG sector 54 multi-collector instrument, using the
122 double spike technique with the calibrated Southampton-Brest $^{207}\text{Pb}/^{204}\text{Pb}$ spike (Ishizuka et
123 al., 2003). The true Pb isotopic compositions were obtained from the natural and mixture runs
124 by iterative calculation adopting a modified linear mass bias correction (Johnson and Beard,
125 1999). The reproducibility of this Pb isotopic measurement (external error: 2σ) by double
126 spike is < 200 ppm for all $^{20x}\text{Pb}/^{204}\text{Pb}$ ratios. Measured values for NBS SRM-981 during the
127 measurement period were $^{206}\text{Pb}/^{204}\text{Pb} = 16.9414 \pm 26$, $^{207}\text{Pb}/^{204}\text{Pb} = 15.4997 \pm 30$ and
128 $^{208}\text{Pb}/^{204}\text{Pb} = 36.726 \pm 9$ (2σ , $n = 9$). Pb blanks measured using this procedure were < 100 pg,
129 and thus negligible relative to the amount of sample analysed.

130
131

132 **3. Geological setting and K-Ar ages**

133

134 *3.1. Geological and tectonic framework*

135

136 The geology of the Republic of Djibouti records the effects of the activity of the Afar
137 mantle plume since 30 Ma (Schilling, 1973; Barberi et al., 1975; Barberi and Varet, 1977;

138 Furman et al., 2006). Plume-related basaltic and derived magmas, variably enriched in
139 incompatible elements (e.g., Joron et al., 1980; Deniel et al., 1994) cover ca. 90% of its
140 surface, and range in age from at least 23.6 ± 0.5 Ma to Present (Barberi et al., 1975;
141 Courtillot et al., 1984; Zumbo et al., 1995). Since the Miocene, the most salient tectono-
142 magmatic process observed in the area was the penetration of the Gulf of Aden (GA) oceanic
143 ridge between the Arabia and Somalia plates, hence leading to the opening of the Tadjoura
144 Gulf (Courtillot et al., 1980; Manighetti et al., 1997), at the southwestern edge of which the
145 emerged Asal Rift shows spectacular [evidence](#) for both tectonic and magmatic activities
146 (Stieltjes et al., 1976; Needham et al., 1976).

147 Onland, the principal marker of the Pliocene opening of the Tadjoura Gulf (TG) was the
148 emplacement of a < 350 m-thick basaltic lava flow pile, referred to as the “initial basaltic
149 series from the borders of the Tadjoura Gulf” (Fournier et al., 1982; Gasse et al., 1983), which
150 will be named hereafter the Tadjoura Gulf Basalts (TGB). These very fluid subaerial lava
151 flows are generally assumed to have been emitted from now submerged fissures in the Gulf,
152 and emplaced rather symmetrically outwards on the twin margins (Fig. 1, inset) (Richard,
153 1979). Additional feeder dykes, and associated neck-like features, have been identified
154 onshore, along the northern flank in the Tadjoura area. TGB range from olivine tholeiites to
155 ferrobasalts, and in thin section are subaphyric to sparsely phyric, with 3-6 modal% calcic
156 plagioclase, and 1-3 modal% olivine set in a microlitic groundmass. They display mild, but
157 significant, enrichments in light rare earth elements (LREE) and other highly incompatible
158 elements (Joron et al., 1980; Barrat et al., 1990, 1993; Deniel et al., 1994).

159 In the Djibouti plain, the TGB are [involved in a coastal network](#) of Gulf-parallel tilted
160 fault blocks, bounded by dominantly extensional N-facing structures, in association with
161 N140°E normal faults outlined by a swarm of small cinder cones (Fig. 1). To the East, they
162 are post-dated by the Hayyabley elongated volcano, the long axis of which also strikes NW-
163 SE, parallel to the regional fault scarp bounding the eastern coastal plain further SE.

164

165 *3.2. The Hayyabley volcano*

166

167 The youngest volcanic units in the Djibouti plain are a set of generally small (less than
168 100 m high) ash and cinder strombolian-type cones with associated basaltic flows (e.g. the
169 Nagâd volcano, Fig. 1), aligned along a young NNW-SSE fracture network (Fournier et al.,
170 1982). They overlie the TGB and have been dated to 1.75-1.70 Ma (Gasse et al., 1983). The
171 largest of these post-TGB volcanic centers is the Hayyabley volcano, east of Djibouti town

172 (Fig. 1). Although it was shown on the 1:50 000 geological map of Djibouti (Fournier et al.,
173 1982), and further well-described and dated by Gasse et al. (1983), it was apparently never
174 investigated later despite the obviously unusual characteristics of its basaltic lavas.

175 The Hayyabley volcano in map-view is a 5x10 km elliptic edifice, with a NNW-SSE
176 trending axis. It has a shield-like and rather flat morphology, and culminates at 147 m at
177 Signal Bouêt. It overlies the TGB lava flows outcropping W and N of Wadi Ambouli valley
178 (Fig. 1), and seals the EW to WNW-ESE normal fault pattern related to the Tadjoura rift.
179 Despite the rather large aerial extent of its lavas, we estimate its volume to ca. 0.6-0.8 km³
180 only. Its eruptive vents are no longer identifiable, possibly because of the strong anthropic
181 imprint and constructions of the Djibouti suburbs: they are thought to be located in its summit
182 zone, and aerial photograph data suggest radial emplacement of the lava flows away from this
183 summit (Fournier et al., 1982).

184 The total thickness of the Hayyabley lava flow pile is estimated at 120 m. The best
185 section is exposed in Wadi Warabor, along the northern coast (Fig. 1). There, **we sampled**
186 **seven** superimposed basaltic lava flows (DJ54B to DJ54H), resting conformably upon a 15 m-
187 thick columnar-jointed lava flow (DJ54A) belonging to the TGB sequence. These flows are
188 vesicle-rich, and their thickness decreases upwards from ca. 4 m to **less than 20 cm**. Only the
189 thickest lava flows show columnar jointing, **and the uppermost ones are highly vesicular and**
190 **often scoriaceous** (Gasse et al., 1983). A sample (TF 914) collected from a possible eruption
191 vent in the summit area had been dated by the K-Ar unspiked method to 0.98 ± 0.10 Ma and
192 0.83 ± 0.08 Ma (Gasse et al., 1983), the youngest K-Ar dates obtained so far in the area. We
193 have checked the previous results by dating two basaltic flows from the Wadi Warabor
194 section (Fig. 1). The results are shown in Table 1. The two ages obtained, 0.93 ± 0.06 Ma and
195 1.06 ± 0.09 Ma, are mutually consistent, and compatible as well with those previously
196 published (Gasse et al., 1983). Indeed, the four results almost overlap at around 0.91 – 0.97
197 Ma, and are remarkably convergent considering the very low concentration of potassium in
198 the studied samples and the young age range.

199

200

201 **4. Petrologic and geochemical results**

202

203 *4.1. Petrographic and mineralogical features*

204

205 The Hayyabley basalts are rather homogeneous from a petrographic point of view, and
206 also quite different from the underlying TGB. They are moderately to highly vesicular (10 to
207 30 modal% vesicles in thin section). These vesicles are usually empty, or sometimes partly
208 filled by calcite, especially in the summit part of the volcano. The rocks are also sparsely to
209 moderately phyrlic, with 5 to 15 modal% phenocrysts, the size of which ranges from 0.5 to 3
210 mm. They include olivine (dominant) and calcic plagioclase (subordinate), in a roughly 2:1
211 ratio. These phenocrysts are set in a holocrystalline groundmass, showing doleritic or
212 intersertal textures. It contains, by order of decreasing abundance, plagioclase laths, olivine
213 microcrysts (the periphery of which is often replaced by iddingsite), calcic pyroxene grains
214 and titanomagnetite.

215 Olivine compositions range from Fo₈₄₋₈₂ for the phenocryst cores to Fo₇₈₋₅₄ for their rims
216 and the microcrysts, the smallest ones being the most Fe-rich. The plagioclase phenocryst
217 cores are bytownitic (An₈₆₋₇₇) and contain negligible amounts of Or component (<0.3%). The
218 corresponding rims are less calcic (An₇₀₋₃₂) and the small laths from the groundmass are
219 clearly enriched in alkalis (up to An₂₇₋₁₅ Ab₇₀₋₈₀ Or₂₋₅). Groundmass clinopyroxenes are augitic
220 (Wo₄₅₋₄₁ En₄₃₋₄₀ Fs₁₂₋₁₆) and their low TiO₂ (<1 wt%) and Na₂O (<0.3 wt%) contents are
221 typical of tholeiitic clinopyroxenes.

222

223 *4.2. Major and trace elements on bulk rocks*

224

225 Nine samples taken from different flows from four locations (Fig. 1) were analysed, and
226 the results are given in Table 2. Their major and trace element abundances are rather uniform.
227 These lavas display high Al₂O₃ (16.4-17.05 wt%) and CaO (12.5-13.8 wt%) abundances, low
228 Na₂O (1.9-2.1 wt%) abundances and FeO*/MgO ratios close to 1. Although not primitive,
229 these lavas are amongst the least evolved basalts collected so far from the Republic of
230 Djibouti. Indeed, they exhibit the highest compatible trace element abundances (e.g., Ni, Co,
231 Cr) measured in samples from this area (e.g., Joron et al., 1980; Barrat et al., 1990, 1993;
232 Deniel et al., 1994).

233 More importantly, their incompatible trace element abundances are low, and these
234 samples are characterized by light REE depletions (La_n/Sm_n=0.76-0.83), and small but
235 significant positive Eu anomalies (Eu/Eu*=1.08-1.12, Fig. 2). These features unambiguously
236 distinguish the Hayyabley basalts from both the TGB and the older post-TGB basalts, which
237 are always LREE-enriched (Joron et al., 1980; Barrat et al., 1990, 1993; Deniel et al., 1994).

238 The unusual features of the Hayyabley basalts are strengthened by their primitive mantle
239 normalised patterns that exhibit large positive Ba ($Ba_n/Rb_n=2.9-8.6$) and Sr ($Sr_n/Ce_n=1.8-2.1$)
240 anomalies (Fig. 3). Although LREE-depleted, the Hayyabley basalts are clearly distinct from
241 typical N-MORB and basalts erupted by the nearby nascent oceanic ridges. For example,
242 basalts with N to T-MORB affinities are known from the eastern part of the Tadjoura Gulf
243 (Barrat et al., 1990, 1993). Although a positive Sr anomaly has been observed in a single
244 LREE-depleted basalt, positive Ba and Eu anomalies are missing (Barrat et al., 1990, 1993
245 and unpublished results). In addition, the Nb/Y and Zr/Y ratios (0.11-0.15 and 2.20-2.57,
246 respectively, Table 2) of Hayyabley basalts are such that these lavas plot within the field of
247 Icelandic plume basalts, and well above the N-MORB field, in Fitton et al.'s (1997, 2003)
248 rectangular plot (not shown).

249 Interestingly, the Hayyabley basalts are remarkably similar to the scarce LREE-depleted
250 basalts which were sporadically emitted by the Manda Hararo rift, Ethiopia (Barrat et al.,
251 2003). Indeed, the latter display incompatible element abundances and distributions very
252 similar to those of the Hayyabley basalts (Fig. 3). The noticeable differences are minor. The
253 Manda Hararo basalts are somewhat more evolved than the Hayyabley basalts and have for
254 example lower Ni and Cr concentrations (Table 3). In addition, an Oligocene basaltic flow
255 with the same features (sample E88) was reported by Pik et al. (1999) from the Ethiopian
256 Plateau.

257

258 4.3. Sr, Nd, Pb isotopic data

259

260 The isotopic compositions of five samples are given in Table 4, and are almost uniform,
261 with the exception of $^{87}Sr/^{86}Sr$ ratios which vary significantly in the range 0.70369 - 0.70396
262 (Table 4). Although relatively fresh, the Hayyabley basalts display some evidence of
263 weathering. One may suspect that their $^{87}Sr/^{86}Sr$ ratios are not pristine, and have been affected
264 by secondary processes. Indeed, the least radiogenic sample DJ59 displays a negative Loss On
265 Ignition (LOI) value (-0.38 wt%). Conversely, the LOI value of the most radiogenic sample
266 (DJ54H) is much higher (0.92 wt%), and in a $^{87}Sr/^{86}Sr$ vs. LOI plot (not shown), a weak
267 positive correlation is apparent. In order to check if the Sr isotopic compositions of the
268 samples were modified by alteration, 150 mg of sample DJ54B was leached for 2 hours in hot
269 (150°C) 6N HCl, and rinsed in deionized water prior to dissolution. Its $^{87}Sr/^{86}Sr$ ratio is
270 significantly lower than the value obtained on the unleached powder (Table 4), a result which

271 suggests that the Sr isotopic compositions have been modified by secondary processes.
272 Similar observations were made by Deniel et al. (1994) on other samples from Djibouti. Thus,
273 $^{87}\text{Sr}/^{86}\text{Sr}$ obtained on unleached samples from this area should be discussed only with extreme
274 caution, even ratios obtained from apparently fresh basalts. We believe that only two $^{87}\text{Sr}/^{86}\text{Sr}$
275 measurements can be safely used in the discussion: the least radiogenic one (DJ59), and the
276 value obtained on the leached residue of DJ54B.

277 The Sr, Nd, and Pb isotopic compositions of the Hayyabley basalts are compared to
278 those of other volcanics from the Horn of Africa in figures 4 to 6. In these plots, Hayyabley
279 basalts lie significantly outside the fields defined by the submarine basalts erupted from the
280 nascent oceanic ridges of the Red Sea, the Eastern part of the Tadjoura Gulf, and the Aden
281 Gulf. These features indicate that these LREE-depleted lavas are unlike MORB (Figs. 5 and
282 6). For example, they display $^{87}\text{Sr}/^{86}\text{Sr}$ ratios more radiogenic than N-MORB, and
283 significantly lower ϵ_{Nd} values (Ito et al., 1987). In contrast, the ϵ_{Nd} vs. $^{87}\text{Sr}/^{86}\text{Sr}$ plot (Fig. 4)
284 shows that the Hayyabley basalts and LREE-depleted basalts from Manda Hararo are
285 isotopically very similar. The Hayyabley basalts display almost uniform Pb isotopic
286 compositions ($^{206}\text{Pb}/^{204}\text{Pb}= 18.47\text{-}18.55$, $^{207}\text{Pb}/^{204}\text{Pb}= 15.52\text{-}15.57$, $^{208}\text{Pb}/^{204}\text{Pb}= 38.62\text{-}38.77$)
287 well above the NHRL (Hart, 1984, 1988; see Table 4). In the Sr-Nd, Pb-Pb and Nd-Pb plots
288 (Figs. 4 to 6), the Hayyabley basalts extend the range of the compositions displayed by the
289 young (< 4 Ma) basalts from Djibouti. They might reflect the contribution of a distinct LREE
290 component in their petrogenesis.

291

292 5. Discussion

293

294 Although Ethiopian Plateau basalts (Pik et al., 1999; Kieffer et al., 2004; Meshesha and
295 Shinjo, 2007; Beccaluva et al., 2009), and Afar basalts (Treuil and Joron, 1975; Joron et al.,
296 1980; Deniel et al., 1994) are dominantly enriched, previous studies (Barrat et al., 1993, 2003;
297 Pik et al., 1999; Meshesha and Shinjo, 2007) have demonstrated that minor depleted
298 components were also involved in their petrogenesis. The discovery of a new occurrence of
299 LREE-depleted basalts in Djibouti, i.e. further east in the Afar rift setting, might provide new
300 constrains on their origin. Two main points will be discussed below: (1) the origin of the Ba,
301 Sr and Eu positive anomalies observed in the Hayyabley basalts, and (2) the occurrence of a
302 specific LREE-depleted component in the sources of the Afar basalts.

303

304 5.1. The Ba, Sr and Eu positive anomalies in the Hayyabley basalts

305

306 The origin of Ba, Sr and Eu positive anomalies in LREE-depleted basalts has been
307 previously investigated in the cases of some Icelandic basalts (e.g., Kokfelt et al., 2006 and
308 references therein) and of the Manda Hararo basalts (Barrat et al., 2003). The compositions of
309 LREE-depleted basalts such as those erupted by the Hayyabley volcano might be related to
310 those of common MORB. The chief differences between them could be due to secondary
311 processes, such as hot-desert weathering, crystal accumulation, or contamination by a crustal
312 component. Alternatively, they could be derived from an unusual mantle source, located in
313 the lithospheric or asthenospheric mantle or in the plume itself.

314 In a hot-desert environment, surface processes are able to generate positive Ba and Sr
315 anomalies in a very short time. The studies of meteorites from Sahara have demonstrated that
316 some of them, and not only the most weathered ones, exhibit marked Ba and Sr enrichments
317 that are sensitive indicators of the development of secondary calcite, gypsum, or barytes (e.g.,
318 Barrat et al., 1998, 2003). Such processes would have generated a range of Ba and Sr
319 abundances from low values typical of unweathered N-MORB (about 10 ppm Ba and 100
320 ppm Sr) to much higher concentrations. However, Ba and Sr abundances in the Hayyabley
321 basalts are uniform, and strikingly similar to the concentrations measured in the distant
322 Manda Hararo basalts. Furthermore, the development of secondary phases is unable to
323 increase the Eu/Eu* ratio and to generate positive Eu anomalies, hence ruling out this first
324 explanation.

325 Positive Ba, Sr and Eu anomalies in basaltic rocks are usually explained by plagioclase
326 accumulation or assimilation. However this process is unable to produce Sr anomalies as high
327 as those displayed by the Hayyabley or Manda Hararo basalts without increasing drastically
328 the Al₂O₃ contents of the resulting rocks. The fact that the Al₂O₃ abundances of the LREE-
329 depleted basalts are not anomalously high (Table 2) is inconsistent with the hypothesis of
330 plagioclase accumulation. Assimilation of [plagioclase-rich gabbros from the oceanic
331 lithosphere](#) during ascent of plume-related magmas has been proposed in the cases of [offshore
332 Tadjoura Gulf basalts](#) (Barrat et al., 1993) and Galapagos basalts (Saal et al., 2007). [However,
333 reproducing the compositions of Hayyabley basalts through this process, and especially their
334 positive Ba, Sr and Eu anomalies, would require rather high rates of assimilation. In addition,
335 the Hayyabley and Manda Hararo basalts overlie thinned continental crust which is 25-26 km
336 thick \(Dugda and Nyblade, 2006\), while the depleted plateau basalt sample E88 \(Pik et al.,
337 1999\) is located on normal \(ca. 40 km thick\) African crust. Due to the presence of a
338 substantial plume-related basaltic cover in both cases, one may expect the occurrence at](#)

339 crustal or even subcrustal depths of associated gabbroic cumulates. However, these gabbros
340 should be LREE-enriched like the vast majority of Afar basalts. Therefore, their interaction
341 with depleted (N-MORB type) melts is likely to lead to variably LREE-enriched magmas with
342 isotopic compositions close to those of the flood basalts.

343 The Hayyabley basalts have radiogenic Sr isotopic compositions and low ϵ_{Nd} values
344 relative to Aden Gulf or Red Sea MORBs (Schilling et al., 1992; Volker et al., 1993; Hase et
345 al., 2000). The assimilation of a continental component could explain this shift from usual N-
346 MORB values, but incompatible trace element ratios give no support to this interpretation.
347 Contamination of MORB-like melts by continental crust would produce significant changes in
348 incompatible trace element ratios. The Hayyabley basalts, like the Manda Hararo LREE-
349 depleted basalts, lack the negative Nb or Ta anomalies observed in the multi-element plots of
350 crust-contaminated basalts. Moreover, they show a limited range of Ce/Pb ratios from 24 to
351 28, similar to values measured in oceanic basalts (e.g., Sun and McDonough, 1989).
352 Therefore, there is no indication for assimilation of significant amounts of material derived
353 from the continental crust in the LREE-depleted basalts. In the case of the Manda Hararo
354 basalts, this conclusion is strengthened by their $\delta^{18}\text{O}$ values close to 5.5 ‰, which are typical
355 of mantle composition (Barrat et al., 2003).

356 Another possible explanation of the specific features of Hayyabley and Manda Hararo
357 basalts is that they might result from the interaction between ascending depleted (N-MORB
358 type) melts and the African subcontinental lithospheric mantle. Once again, such a mantle is
359 expected to be LREE-enriched (Hart et al., 1989; Vidal et al., 1991; Deniel et al., 1994) and
360 thus should transmit its trace element and isotopic fingerprint to LREE-poor ascending
361 magmas. In addition, the remarkably similar chemical features of Hayyabley, Manda Hararo
362 and E88 basalts suggest that they derive from almost identical sources and petrogenetic
363 processes. Their distinct locations, emplacement ages (Oligocene for E88, ca. 1 Ma for
364 Hayyabley and less than 0.2 Ma for Manda Hararo) and underlying crustal/lithospheric
365 thickness (normal for E88, thinned for the two other occurrences) are hardly consistent with a
366 similar petrogenetic history.

367 Therefore, as previously pointed out for the Manda Hararo basalts (Barrat et al., 2003),
368 the positive Sr, Ba and Eu anomalies and the particular Sr-Nd-Pb isotopic features of the
369 Hayyabley basalts, are more likely a genuine feature inherited from their deep mantle sources.
370 The same conclusions have been reached for depleted basalts with similar positive anomalies
371 from Iceland. Chauvel and Hémond (2000), Skovgaard et al. (2001), and Kokfelt et al. (2006)
372 have suggested that the sources of Icelandic lavas contained an old recycled oceanic

373 lithosphere component and that melting of the gabbroic portion of this lithosphere led to the
374 formation of basalts that exhibit large positive Ba, Sr and Eu anomalies. At first glance, such
375 an explanation is attractive because if this recycled gabbroic component has been
376 hydrothermally altered, one may expect $^{87}\text{Sr}/^{86}\text{Sr}$ ratios much more radiogenic than those of
377 typical MORB. Hence, the involvement of such component could account for the relatively
378 high $^{87}\text{Sr}/^{86}\text{Sr}$ ratios of the Manda Hararo and Hayyabley depleted basalts. However, an old
379 LREE-depleted recycled gabbroic component from the oceanic lithosphere would also be
380 characterized by high ϵ_{Nd} values. On the contrary, the Manda Hararo and Hayyabley lavas
381 display ϵ_{Nd} values unexpectedly low ($\epsilon_{\text{Nd}} = 5-7$) for depleted basalts. Thus, we conclude that,
382 at best, this model only partially fits the observations.

383

384 *5.2. The depleted components in the sources of Djibouti and Ethiopian basalts*

385

386 Previous geochemical studies have demonstrated the participation of a depleted
387 component during the genesis of the Horn of Africa basalts. In the case of basalts emitted by
388 the young oceanic ridges from the Red Sea or the Aden Gulf, major involvement of MORB-
389 related sources has been proposed (e.g., Barrat et al., 1990, 1993; Schilling et al., 1992;
390 Volker et al., 1993). These submarine basalts do not have the unradiogenic Pb isotopes of the
391 Carsberg Ridge ca. 1600 km east of Hayyabley volcano (Hart, 1984) but do extend away
392 from the Indian Ocean MORB toward a more HIMU composition. On land, huge volumes of
393 enriched basalts were emplaced in Afar and Ethiopia. The trace element and isotopic features
394 of the depleted reservoirs which have been involved during the genesis of the scarce LREE-
395 depleted lavas are very difficult to constrain. Two distinct LREE-depleted components have
396 been unambiguously detected.

397 First, a depleted MORB mantle component is clearly involved in the genesis of
398 Quaternary basalts from Northern Afar. The Sr-Nd-Pb isotopic relationships displayed by the
399 Erta' Ale basalts (Figs. 4 to 6) point to the participation of two mantle end-members, namely a
400 HIMU component and a depleted mantle (DM) component undistinguishable from the source
401 of the Red Sea MORB (Barrat et al., 1998). Furthermore, a similar depleted component has
402 been detected in the sources of the Oligocene lavas from the Northwestern Ethiopian volcanic
403 province (Meshesha and Shinjo, 2007). The entrainment of depleted asthenospheric mantle
404 during plume ascent (Furman et al., 2006) is a possible explanation for the contribution of this
405 component to the sources of some of the basalts erupted in Afar and Ethiopia, as well as to
406 those of Kerguelen basalts (Doucet et al., 2002). However, numerical models (Farnetani et al.,

407 2002; Farnetani and Samuel, 2005) suggest that incorporation of depleted upper mantle within
408 ascending plumes is unlikely to occur.

409 In addition, the compositions of LREE-depleted basalts from Hayyabley and Manda
410 Hararo point to a depleted end-member chemically (Fig. 3) and isotopically (Figs. 4 to 6)
411 distinct from an asthenospheric MORB-like component. A single Oligocene LREE-depleted
412 basalt displaying chemical features similar to those of the Quaternary depleted ones has been
413 collected in Ethiopia (sample E88, Pik et al., 1999). Although its isotopic composition is
414 slightly different from those of the Hayyabley basalts (Figs. 4 to 6), the occurrence of this
415 sample indicates that a depleted component distinct from the MORB source was involved in
416 this area at an early stage of plume emplacement. Therefore, we suggest that a depleted
417 component, intrinsic to the plume at depth, has contributed to the sources of both young and
418 old lavas related to the Afar plume. Similar conclusions have been reached for the Hawaiian
419 (Frey et al., 2005) and Icelandic (Thirlwall, 1995; Kerr et al., 1995; Fitton et al., 1997;
420 Chauvel and Hémond, 2000; Thirlwall et al., 2004; Skovgaard et al., 2001; Kokfelt et al.,
421 2006) plumes. However, the nature of this component is currently difficult to constrain in the
422 Afar case. Indeed, melting of the gabbroic part of an old recycled oceanic lithosphere (e.g.,
423 Kokfelt et al., 2006) would produce high ϵ_{Nd} magmas and therefore this process does not
424 account for the low ϵ_{Nd} values of Hayyableh and Manda Hararo basalts. Alternatively, LREE
425 depletion could be due to a previous melting event affecting the plume materials, as proposed
426 by Thirlwall et al. (2004) for their ID2 (or RRD2) depleted component of the Icelandic plume.
427 This hypothesis may account for the Pb isotopic differences between Hayyabley/Manda
428 Hararo basalts and the other (enriched) Djibouti basalts (Figs. 4 to 6) but can hardly explain
429 the higher Sr isotopic ratios of Hayyabley and Manda Hararo basalts.

430 Finally, another intriguing problem is the causal mechanism for the sporadic eruption of
431 small volumes of such nearly pure “depleted” melts in spatially and temporally distinct
432 locations, without any significant contamination by the dominant enriched materials. Indeed,
433 such features are difficult to reconcile with models postulating a large concentrically-zoned
434 Afar plume (e.g., Beccaluva et al., 2009). Numerical simulations of the evolution of thermal
435 and thermo-chemical plumes (Farnetani et al., 2002; Farnetani and Samuel, 2005; Farnetani
436 and Hofmann, 2009) suggest that small heterogeneous mantle domains present in the thermal
437 boundary layer feeding the plume are converted, during the ascent of the latter, into long-lived
438 elongated and narrow filaments within the plume conduit. Such filaments would melt
439 sporadically, and then eventually communicate their specific geochemical fingerprint to small
440 volumes of basaltic lavas (Farnetani and Hoffmann, 2009).

441

442 **6. Conclusions**

443

444 The ~1 Ma-old Hayyabley volcano (SE Djibouti) has emitted ca. 0.6-0.8 km³ of
445 LREE-depleted basalts ($La_n/Sm_n=0.76-0.83$) that display unusual chemical features (positive
446 Ba, Sr and Eu anomalies). These lavas are chemically distinct from the N-MORBs erupted
447 from the nearby Red Sea and Gulf of Aden oceanic ridges, and instead closely resemble the
448 LREE-depleted basalts from the Manda Hararo rift in Central Afar (Barrat et al., 2003).
449 Another similar occurrence, Oligocene in age, has been reported from the trap series in the
450 Ethiopian Plateau by Pik et al. (1999). Our new results confirm the presence within the Afar
451 region of basalts derived from an uncommon depleted component, isotopically distinct from
452 the source of the Red Sea MORBs and from the similarly depleted mantle (DM in Figs. 4 to
453 6) which contributes to the genesis of Erta' Ale volcanics (Barrat et al., 1998). This component
454 is not unusual from an isotopic (Sr, Nd, Pb, O) point of view, and is mainly recognizable from
455 the specific trace element signature of the corresponding basalts (positive Ba, Sr, Eu
456 anomalies combined with LREE depletion).

457 The origin of the Hayyabley-Manda Hararo basalts fingerprint could be ascribed to the
458 interactions between (i) depleted (N-MORB type) basalts derived from an asthenospheric
459 mantle component similar to the Erta 'Ale depleted end-member and (ii) enriched lithospheric
460 materials which would be responsible for the positive Ba, Sr and Eu anomalies. These
461 materials could be either the African continental crust, flood basalt-related gabbroic
462 cumulates stored within or below it, or finally the subcontinental lithospheric mantle.
463 However, all these materials are mostly LREE-enriched, and the contamination hypothesis can
464 hardly explain the clear LREE, Rb and Th depletion and concomitant Ba, Sr and Eu
465 enrichment of Hayyabley basalts (Figs. 2 and 3) as well as their Pb isotopic signature (Figs. 5
466 and 6). Moreover, contamination in plume-related volcanic series is often described as a
467 variable, occasional or random process. Thus, it can hardly account for the very specific trace
468 element and isotopic signature of the Afar depleted basalts, which were erupted in three
469 separate locations, with distinct emplacement ages and underlying crustal/lithospheric
470 thickness.

471 Therefore, our preferred conclusion is that these depleted basalts derive from a intrinsic
472 (although volumetrically minor) depleted component from the Afar plume, possibly present as
473 elongated and narrow filaments within the plume conduit. Sporadic melting of such filaments

474 might account for the restricted spatial and temporal distribution of the Afar depleted basalts.
475 The precise origin of this deep mantle component is currently difficult to constrain, given the
476 small number of depleted basalt samples and the limited amount of corresponding
477 geochemical data. The most likely hypothesis is the contribution of recycled gabbros from
478 ancient oceanic crust.

479

480 **Acknowledgements**

481

482 This study has been funded by the French Embassy in Djibouti, and the grant of the first author (M.A.D.)
483 provided by the MAWARI international program managed by the CIFEG, Orléans, France. Analytical expenses
484 were funded by the MAWARI program and UMR 6538, Plouzané. We especially thank Dr. Mohamed Jalludin,
485 Director of the CERD, for his interest, scientific discussions and logistic support, Ali Abdillahi for his efficiency
486 in organizing fieldwork, and Marcel Bohn for his help with microprobe analysis. [Careful reviews by Tania](#)
487 [Furman and Godfrey Fitton led us to improve significantly the organization and contents of this manuscript.](#)

488

489 **References**

490

491 Baker, J.A., Thirlwall, M.F., Menzies, M.A., 1996. Sr-Nd-Pb isotopic and trace element
492 evidence for crustal contamination of plume-derived flood basalts: Oligocene flood
493 volcanism in Western Yemen. *Geochimica et Cosmochimica Acta* 60, 2559-2581.

494

495 Barberi, F., Ferrara, G., Santacroce, R., Varet, J., 1975. Structural evolution of the Afar
496 triple junction. In: Pilger, A., Rösler, A., (Eds.) *Afar Depression of Ethiopia*.
497 Schweizerbart, Stuttgart, 38-54.

498

499 Barberi, F., Varet, J., 1977. Volcanism in Afar, small scale plate tectonics implications.
500 *Geological Society of America Bulletin* 88, 1251-1266.

501

502 Barrat, J.A., Keller, F., Amossé, J., Taylor, R.N., Nesbitt, R.W., Hirata, T., 1996.
503 Determination of rare earth elements in sixteen silicate reference samples by ICP-MS
504 after Tm addition and ion exchange separation. *Geostandards Newsletter* 20, 133-139.

505

506 Barrat, J.A., Fourcade, S., Jahn, B.M., Cheminée, J.L., Capdevila, R., 1998. Isotope (Sr, Nd,
507 Pb, O) and trace-element geochemistry of volcanics from the Erta'Ale range (Ethiopia).
508 *Journal of Volcanology and Geothermal Research* 80, 85-100.

509

510 Barrat, J.A., Jahn, B.M., Joron, J.L., Auvray, B., Hamdi, H., 1990. Mantle heterogeneity in
511 northeastern Africa: evidence from Nd isotopic compositions and hygromagmaphile
512 element geochemistry of basaltic rocks from the Gulf of Tadjoura and Southern Red Sea
513 regions. *Earth and Planetary Science Letters* 101, 233-247.

514

515 Barrat, J.A., Jahn, B.M., Fourcade, S., Joron, J.L., 1993. Magma genesis in an ongoing
516 rifting zone: the Tadjoura Gulf. *Geochimica et Cosmochimica Acta* 57, 2291-2302.

517

518 Barrat, J.A., Blichert-Toft, J., Gillet, P., Keller, F., 2000. The differentiation of eucrites: the
519 role of *in situ* crystallization. *Meteoritics & Planetary Science* 35, 1087-1100.

520

521 Barrat, J.A., Joron, J.L., Taylor, R.N., Fourcade, S., Nesbitt, R.W., Jahn, B.M., 2003.
522 Geochemistry of basalts from Manda Hararo, Ethiopia: LREE-depleted basalts in
523 Central Afar. *Lithos* 69, p. 1-13.

524

525 Barrat, J.A., Yamaguchi, A., Greenwood, A., Bohn, M., Cotten, J., Benoit, M., Franchi,
526 I.A., 2007. The Stannern trend eucrites: contamination of main group eucritic magmas
527 by crustal partial melts. *Geochimica et Cosmochimica Acta* 71, 4108-4124.

528

529 [Beccaluva, L., Bianchini, G., Natali, C., Siena, F., 2009. Continental flood basalts and
530 mantle plumes: a case study of the Northern Ethiopian Plateau. *Journal of Petrology*
531 \[50, 1377-1403.\]\(#\)](#)

532

533 Blichert-Toft, J., White, W.M., 2001. Hf isotope geochemistry of the Galapagos Islands.
534 *Geochemistry, Geophysics, Geosystems* 2, doi:10.129/2000GC000138.

535

536 Charbit, S., Guillou, H., Turpin, L., 1998. Cross calibration of K-Ar standard minerals using
537 an unspiked Ar measurement technique. *Chemical Geology* 150, 147-159.

538

539 Chauvel, C., Hémond C., 2000. Melting of a complete section of recycled oceanic crust:
540 trace element and Pb isotopic evidence from Iceland. *Geochemistry, Geophysics,*
541 *Geosystems* 1, paper number 1999GC000002.

542

543 Chen, C.-Y., Frey, F.A., 1985. Trace element and isotope geochemistry of lavas from
544 Halaakala Volcano, East Maui: implications for the origin of Hawaiian basalts. *Journal*
545 *of Geophysical Research* 90, 8743-8768.

546

547 Cotten, J., Le Dez, A., Bau, M., Caroff, M., Maury, R.C., Dulski, P., Fourcade, S., Bohn,
548 M., Brousse, R., 1995. Origin of anomalous rare-earth element and yttrium
549 enrichments in subaerially exposed basalts: Evidence from French Polynesia.
550 *Chemical Geology* 119, 115-138.

551

552 Courtillot, V., Galdeano, A., Le Mouel, J.-L., 1980. Propagation of an accreting plate
553 boundary: a discussion of new magnetic data in the Gulf of Tadjoura and Southern Afar.
554 *Earth and Planetary Science Letters* 47, 144-160.

555

556 Courtillot, V., Achache, J., Landre, F., Bonhommet, N., Montigny, R., Féraud, G., 1984.
557 Episodic spreading and rift propagation: new paleomagnetic and geochronologic data
558 from the Afar nascent passive margin. *Journal of Geophysical Research* 89, 3315-3333.

559

560 Daoud, M.A., 2008. Dynamique du rifting continental de 30 Ma à l'Actuel dans la partie
561 sud-est du Triangle Afar. Tectonique et magmatisme du rift de Tadjoura et des
562 domaines Danakil et d'Ali Sabieh, République de Djibouti. Thèse, Université de
563 Bretagne Occidentale, Brest, 190 p.

564

565 Defant, M.J., Maury, R.C., Ripley, E.M., Feigenson, M.D., Jacques, D., 1991. An example
566 of island-arc petrogenesis: geochemistry and petrology of the southern Luzon arc,
567 Philippines. *Journal of Petrology* 32, 455-500.

568

569 Deniel, C., Vidal, P., Coulon, C., Vellutini, P.J., Piguet, P., 1994. Temporal evolution of
570 mantle sources during continental rifting: the volcanism of Djibouti (Afar). *Journal of*
571 *Geophysical Research* 99, 2853-2869.

572

573 Dosso, L., Bougault, H., Joron, J.L., 1993. Geochemical morphology of the North Mid-
574 Atlantic Ridge, 10°-24°N: trace element-isotope complementary. *Earth and Planetary*
575 *Science Letters* 120, 443-462.

576
577
578
579
580
581
582
583
584
585
586
587
588
589
590
591
592
593
594
595
596
597
598
599
600
601
602
603
604
605
606

Doucet, S., Weis, D., Scoates, J.S., Nicolaysen, K., Frey, F.A., Giret, A., 2002. The depleted mantle component in Kerguelen Archipelago basalts: petrogenesis of tholeiitic-transitional basalts from the Loranchet Peninsula. *Journal of Petrology* 43, 1341-1366.

Dugda, M.T., Nyblade, A.A., 2006. New constraints on crustal structure in eastern Afar from the analysis of receiver functions and surface wave dispersion in Djibouti. In: Yirgu, G., Ebinger, C.J., Maguire, P.K.H., (Eds.), *The Afar volcanic province within the East African Rift System*. Geological Society of London, Special Publication 259, 239-251.

Evensen, N.M., Hamilton, P.J., O'Nions, R.K., 1978. Rare Earth abundances in chondritic meteorites. *Geochimica et Cosmochimica Acta* 42, 1199-1212.

Farnetani, C.G., Legras, B., Tackley, P.J., 2002. Mixing and deformation in mantle plumes. *Earth and Planetary Science Letters*, 196, 1-15.

Farnetani, C.G., Samuel, H., 2005. Beyond the thermal plume paradigm. *Geophysical Research Letters*, 32, L07311, doi:10.129/2005GL022360.

Farnetani, C.G., Hofmann, A.W., 2009. Dynamics and internal structure of a lower mantle plume conduit. *Earth and Planetary Science Letters*, 282, 314-322.

Fitton, J.G., Saunders, A.D., Norry, M.J., Hardason, B.S., Taylor, R.N., 1997. Thermal and chemical structure of the Iceland plume. *Earth and Planetary Science Letters*, 153, 197-208.

Fitton, J.G., Saunders, A.D., Kempton, P.D., Hardason, B.S., 2003. Does depleted mantle form an intrinsic part of the Iceland plume? *Geochemistry, Geophysics, Geosystems* 4, 2002GC000424.

607 Fournier, M., Gasse, F., Lépine, J.-C., Richard O., Ruegg J.C., 1982. Carte géologique de la
608 République de Djibouti à 1:100 000. Djibouti. ISERST. Ministère français de
609 Coopération. Ed. ORSTOM, Paris.

610

611 Frey, F.A., Huang, S., Blichert-Toft, J., Regelous, M., Boyet, M., 2005. Origin of depleted
612 components in basalt related to the Hawaiian hot spot: Evidence from isotopic and
613 incompatible element ratios. *Geochemistry, Geophysics, Geosystems* 6, Q02L07,
614 doi:10.129/2004GC000757.

615

616 Fuhrmann, U., Lippolt, H., Hess, J.C., 1987. HD-B1 Biotite reference material for K-Ar
617 chronometry. *Chemical Geology* 66, 41-51.

618

619 Furman, T., Bryce, J., Rooney, T., Hana, B., Yirgu, G., Ayalew, D., 2006. Heads and tails:
620 30 million years of the Afar plume. In: Yirgu, G., Ebinger, C.J., Maguire, P.K.H.,
621 (Eds.), *The Afar volcanic province within the East African Rift System*. Geological
622 Society of London, Special Publication 259, 95-119.

623

624 Gasse, F., Fournier, M., Richard, O., Ruegg, J.C., 1983. Carte géologique de la République
625 de Djibouti à 1:100 000. Djibouti. Notice explicative. ISERST, Ministère français de la
626 Coopération, Ed. ORSTOM, Paris, 70 pp.

627

628 Guillou, H., Singer, B., Laj, C., Kissel, C., Scaillet, S., Jicha, B.R., 2004. On the age of the
629 Laschamp geomagnetic event. *Earth and Planetary Science Letters*, 227, 331-343.

630

631 Hart, S.R., 1984. A large-scale isotope anomaly in the Southern Hemisphere mantle. *Nature*
632 309, 753-757.

633

634 Hart, S.R., 1988. Heterogeneous mantle domains: signatures, genesis and mixing
635 chronologies. *Earth and Planetary Science Letters* 90, 273-296.

636

637 Hart, S.R., Hauri, E.H., Oschmann, L.A., Whitehead, J.A., 1992. Mantle plumes and
638 entrainment: isotopic evidence. *Science* 256, 517-520.

639

640 Hart, W.K., Woldegabriel, G., Walter, R.C., Mertzman, S.A., 1989. Basaltic volcanism in
641 Ethiopia: constraints on continental rifting and mantle interactions. *Journal of*
642 *Geophysical Research* 94, 7731-7748.

643

644 Hase, K.M., Mühe, R., Stoffers, P., 2000. Magmatism during extension of the lithosphere:
645 geochemical constraints from lavas of the Shaban Deep, northern Red Sea. *Chemical*
646 *Geology* 166, 225-239.

647

648 Hémond, C., Arndt, N.T., Lichtenstein, U., Hofmann, A., 1993. The heterogeneous Iceland
649 plume: Nd-Sr-O isotopes and trace element constraints. *Journal of Geophysical*
650 *Research* 98, 15803-15850.

651

652 Hoernle, K., Werner, R., Phipps-Morgan, J., Garbe-Schönberg, D., Bryce, J., Mrazek, J.,
653 2000. Existence of complex spatial zonation in the Galapagos plume for at least 14 m. y.
654 *Geology* 28, 435-438.

655

656 Ishizuka, O., Taylor, R.N., Milton, J.A., Nesbitt, R.W., 2003. Fluid-mantle interaction in an
657 intraoceanic arc: constraints from high-precision Pb isotopes. *Earth and Planetary*
658 *Science Letters* 211, 221-236.

659

660 Ito, E., White, W.M., Göpel, C., 1987. The O, Sr, Nd, and Pb isotope geochemistry of
661 MORB. *Chemical Geology* 62, 157-176.

662

663 Joron, J.L., Treuil, M., Jaffrezic, H., Villemant, B., Richard, O., 1980. Géochimie des
664 éléments en traces du volcanisme de l'Afar et de la mégastructure Mer Rouge-Afar-
665 Golfe d'Aden. Implications pétrogénétiques et géodynamiques. *Bulletin de la Société*
666 *géologique de France* (7) 22, 945-957.

667

668 Johnson, C.M., Beard, B.L., 1999. Correction of instrumentally produced mass
669 fractionation during isotopic analysis of Fe by thermal ionization mass spectrometry,
670 *International Journal of Mass Spectrometry* 193, 87-99.

671

672 Kerr, A.C., Saunders, A.D., Tarney, J., Berry, N.H., Hards, V.L., 1995. Depleted mantle-
673 plume geochemical signatures: No paradox for plume theories. *Geology* 23, 843-846.

674
675
676
677
678
679
680
681
682
683
684
685
686
687
688
689
690
691
692
693
694
695
696
697
698
699
700
701
702
703
704
705
706

- Kokfelt, T.F., Hoernle, K., Hauf, F., Fiebig, J., Werner, R., Garbe-Schomberg, D., 2006. Combined trace element and Pb-Nd-Sr-O isotope evidence for recycled oceanic crust(upper and lower) in the Iceland mantle plume. *Journal of Petrology* 47, 1705-1749.
- Laughlin, A.W., Poths, S., Healey, H., Reneau, S., Woldegabriel, G., 1994. Dating Quaternary basalts using the ^3He and ^{14}C methods with implications for excess Ar. *Geology* 22, 135-138.
- Lin, S.-S., Keken, P.E. van, 2006. Dynamics of thermochemical plumes: 2. Complexity of plume structures and its implications for mapping mantle plumes. *Geochemistry, Geophysics, Geosystems* 7, Q033003, doi:10.129/2005GC001072.
- Manighetti, I., Tapponnier, P., Courtillot, V., Gruszow, S., Gillot., P.Y., 1997. Propagation of rifting along the Arabia-Somalia plate boundary: the Gulfs of Aden and Tadjoura. *Journal of Geophysical Research* 102, 2681-2710.
- Meshesha, D., Shinjo, R., 2007. Crustal contamination and diversity of magma sources in the Northwestern Ethiopian volcanic province. *Journal of Mineralogical and Petrological Sciences*, 102, 272-290.
- Needham, H.D., Choukroune, P., Cheminée, J.-L., Le Pichon, X., Francheteau, J., Tapponnier, P., 1976. The accreting plate boundary: Ardoukobâ Rift (N.E. Africa) and the oceanic Rift valley. *Earth and Planetary Science Letters* 28, 439-453.
- Odin, G.S., and 35 collaborators, 1982. Interlaboratory standards for dating purposes. In: Odin G.S., (Ed.), *Numerical dating in stratigraphy*, Wiley, Chichester, 123-149.
- Pik, R., Deniel, C., Coulon, C., Yirgu, G., Hoffmann, C., Ayalew, D., 1998. The northwestern Ethiopian Plateau flood basalts: Classification and spatial distribution of magma types. *Journal of Volcanology and Geothermal Research* 81, 91-111.

707 Pik, R., Deniel, C., Coulon, C., Yirgu, G., Marty, B., 1999. Isotopic and trace element
708 signatures of Ethiopian flood basalts: evidence for plume-lithosphere interactions.
709 *Geochimica et Cosmochimica Acta* 63, 2263-2279.
710

711 Richard, O. 1979. Etude de la transition dorsale océanique – rift émergé: le golfe de
712 Tadjoura (République de Djibouti). Approche géologique, géochronologique et
713 pétrologique. Thèse 3^{ème} cycle, Université de Paris XI-Orsay, 149 p.
714

715 Rogers, N.W., 2006. Basaltic magmatism and the geodynamics of the East African Rift
716 System. In: Yirgu, G., Ebinger, C.J., Maguire, P.K.H., (Eds.), *The Afar volcanic
717 province within the East African Rift System*. Geological Society of London, Special
718 Publication 259, 77-93.
719

720 Saal, A.E., Kurtz, M.D., Hart, S.R., Blusztajn, J.S., Blichert-Toft, J., Liang, Y., Geist, D.J.,
721 2007. The role of lithospheric gabbros on the composition of Galapagos lavas. *Earth
722 and Planetary Science Letters* 257, 391-406.
723

724 Scaillet, S., Guillou, H., 2004. A critical evaluation of young (near-zero) K-Ar ages. *Earth
725 and Planetary Science Letters* 220, 265-275.
726

727 Schilling, J.G., 1973. Afar mantle plume: rare earth evidence. *Nature* 242, 2-5.
728

729 Schilling, J.G., Kingsley, R.H., Hanan, B.B., McCully, B.L., 1992. Nd-Sr-Pb variations
730 along the Gulf of Aden: evidence for Afar Mantle plume-continental lithosphere
731 interaction. *Journal of Geophysical Research* 97, 10927-10966.
732

733 Skovgaard, A.C., Storey, M., Baker, J., Blusztajn, J., Hart, S.R., 2001. Osmium-oxygen
734 isotopic evidence for a recycled and strongly depleted component in the Iceland mantle
735 plume. *Earth and Planetary Science Letters* 194, 259-275.
736

737 Steiger, R.H., Jäger, E., 1977. Subcommittee on geochronology: convention on the use of
738 decay constants in geo- and cosmochemistry. *Earth and Planetary Science Letters* 36,
739 359-362.
740

741 Stieltjes, L., Joron, J.L., Treuil, M., Varet, J., 1976. Le rift d'Asal, segment de dorsale
742 émergée: discussion pétrologique et géochimique. Bulletin de la Société géologique de
743 France (7) 18, 851-862.
744

745 Sun, S.S., McDonough, W.F., 1989. Chemical and isotopic systematics of oceanic basalts:
746 Implications for mantle composition and processes. In: Saunders, A.D., Norry, M.J.,
747 (Eds.), Magmatism in the ocean basins. Geological Society of London Special
748 Publication 42, 313-345.
749

750 Taylor, R.N., Thirlwall, M.F., Murton, B.J., Hilton, D.R., Gee, M.A.M., 1997. Isotopic
751 constraints on the influence of the Icelandic plume. Earth and Planetary Science Letters
752 148, 1-8.
753

754 [Thirlwall, M.F., 1995. Generation of the Pb isotopic characteristics of the Iceland plume.
755 Journal of the Geological Society of London, 152, 991-996.](#)
756

757 Thirlwall, M.F., Gee, M.A.M., Taylor, R.N., Murton, B.J., 2004. Mantle components in
758 Iceland and adjacent ridges investigated using double-spike Pb isotope ratios.
759 Geochimica et Cosmochimica Acta 68, 361-386.
760
761

762 Treuil, M., Joron, J.L., 1975. Utilisation des éléments hygromagmatophiles pour la
763 simplification de la modélisation quantitative des processus magmatiques. Exemples de
764 l'Afar et de la dorsale médioatlantique. Rendiconti della Società Italiana di Mineralogia
765 e Petrologia 31, 125-174.
766

767 Vidal, P., Deniel, C., Vellutini, P.J., Piguet, P., Coulon, C., Vincent, J., Audin, J., 1991.
768 Changes of mantle sources in the course of a rift evolution: the Afar case. Geophysical
769 Research Letters 18, 1913-1916.
770

771 Volker, F., Altherr, R., Jochum, K.P., McCulloch, M.T., 1997. Quaternary volcanic activity
772 of the southern Red Sea: new data and assessment of models on magma sources and
773 Afar plume-lithosphere interaction. Tectonophysics 278, 15-29.
774

- 775 Volker, F., McCulloch, M.T., Altherr, R., 1993. Submarine basalts from the Red Sea: new
776 Pb, Sr, and Nd isotopic data. *Geophysical Research Letters* 20, 927-930.
777
- 778 White, W.M., McBirney, A.R., Duncan, R.A., 1993. Petrology and geochemistry of the
779 Galapagos islands: portrait of a pathological mantle plume. *Journal of Geophysical*
780 *Research* 98, 19533-19563.
781
- 782 Yang, H.-J., Frey, F.A., Clague, D.A., 2003. Constraints on the source components of lavas
783 forming the Hawaiian North Arch and Honolulu volcanoes. *Journal of Petrology* 44,
784 603-627.
785
- 786 Yurtmen, S., Guillou, H., Orhan, O., Rowbotham, G., Westaway, R., 2002. Rate of strike-
787 slip on the Amanos Fault (Karasu Valley, southern Turkey) constrained by K-Ar dating
788 and geochemical analysis of Quaternary basalts. *Tectonophysics* 344, 207-246.
789
- 790 Zindler, A., Hart, S.R., Frey, F.A., Jakobsson, S.P., 1979. Nd and Sr isotope ratios and rare
791 earth abundances in Reykjanes Peninsula basalts: evidence for mantle heterogeneity
792 beneath Iceland. *Earth and Planetary Science Letters* 45, 249-262.
793
- 794 Zumbo, V., Féraud, G., Vellutini, H., Pigué, P., Vincent, J., 1995. First $^{40}\text{Ar}/^{39}\text{Ar}$ dating on
795 Early Pliocene to Plio-Pleistocene magmatic events of the Afar – Republic of Djibouti.
796 *Journal of Volcanology and Geothermal Research* 65, 281-295.
797

798 **Figure captions**

799
800 Fig. 1. Geological setting of the Djibouti Plain. (a) Location of the study area in the Tadjoura
801 Gulf context. (b) ASTER satellite image showing the Hayyabley volcano post-dating the
802 coastal fault belt related to the Tadjoura rift. (c) Geological interpretation of Fig. 1b.
803

804 Fig. 2. Chondrite-normalized REE patterns of Hayyableh basalts compared to the field of
805 older Tadjoura Gulf basalts [located onland in Djibouti](#) (Barrat et al., 1993; Daoud, 2008). The
806 reference chondrite is from Evensen et al. (1978). [The pattern of a southern Red Sea N-](#)
807 [MORB \(sample V84, Barrat et al., 1990\) is shown for comparison.](#)
808

809 Fig. 3. Primitive mantle-normalized element patterns for Hayyabley basalts, LREE-depleted
810 Manda Hararo basalts (Barrat et al., 2003), two submarine MORB from the East of the Gulf
811 of Tadjoura (Barrat et al., 1990, 1993), the southern Red Sea N-MORB sample V84 (Barrat
812 et al., 1990), and the LREE-depleted sample E88 from the Oligocene Ethiopian Plateau (Pik
813 et al., 1999). The primitive mantle values are from Sun and McDonough (1989).

814

815 Fig. 4. Plot of ϵ_{Nd} vs. $^{87}Sr/^{86}Sr$ for young onland basalts from Djibouti (Deniel et al., 1994, and
816 this study). Only the two reliable Sr isotopic ratios of Hayyabley basalts have been plotted.
817 Basalts older than 4 Ma have been omitted because of their possible contamination by
818 continental crust. The fields of (1) basalts from the South Red Sea occurrences, which include
819 oceanic ridge segments, Ramad seamount and Zubair and Hanish islands (Barrat et al., 1990,
820 1993; Volker et al., 1993, 1997), (2) submarine basalts from the East of the Gulf of Tadjoura
821 and the Aden Gulf (Barrat et al., 1990, 1993; Schilling et al., 1992), (3) Erta 'Ale volcanics
822 (Barrat et al., 1998), (4) LREE-depleted basalts from Manda Hararo (MH, Barrat et al., 2003),
823 and (5) some Ethiopian samples (E88: depleted Oligocene basalt; HT2: average composition
824 of high-Ti basalts, Pik et al., 1999) are shown for comparison. DM refers to the regional
825 depleted mantle composition deduced from the study of South Red Sea and Gulf of Aden
826 basalts.

827

828 Fig. 5. Plot of $^{207}Pb/^{204}Pb$ and $^{208}Pb/^{204}Pb$ vs. $^{206}Pb/^{204}Pb$ for young (less than 4 Ma) onland
829 enriched basalts from Djibouti (Deniel et al., 1994) and Hayyabley depleted basalts (this
830 study). Other fields as in Fig. 4. E'A: field of Erta 'Ale volcanics (Barrat et al., 1998). Most
831 $^{207}Pb/^{204}Pb$ data taken from the regional literature (e.g. on E88 and Erta 'Ale) are less precise
832 than those measured on Hayyabley basalts, and should therefore be considered with caution.

833

834 Fig. 6. Plot of $^{206}Pb/^{204}Pb$ vs. ϵ_{Nd} for young (less than 4 Ma) onland enriched basalts from
835 Djibouti (Deniel et al., 1994) and Hayyabley depleted basalts (this study). Other fields as in
836 Fig. 5.

837

838 **Table captions**

839

840 Table 1. Unspiked ^{40}K - ^{40}Ar datings of Hayyabley basalts. See text for the analytical
841 procedures.

842

843 Table 2. Major and trace element analyses of Hayyabley basalts (major oxides in wt%, trace
844 elements in ppm). ICP-AES and ICP-MS analytical methods described in the text.

845

846 Table 3. Compositions of LREE-depleted basalts from Hayyabley (average of the samples
847 analysed by ICP-MS), Manda Hararo (average data from Barrat et al., 2003), Ethiopian
848 Plateau (sample E88, Pik et al., 1999), and of a N-MORB from Tadjoura Gulf (sample A3D3,
849 Joron et al., 1980; Barrat et al., 1993). Major oxides in wt%, trace elements in ppm. n denotes
850 ratios normalized to the primitive mantle composition from Sun and McDonough (1989).

851

852 Table 4. Sr, Nd and Pb isotopic compositions of Hayyabley basalts (B: bulk rock; R: residue
853 after leaching). See text for the analytical procedures. $\Delta 7/4$ and $\Delta 8/4$ denote the deviation (in
854 ‰) of $^{207}\text{Pb}/^{204}\text{Pb}$ and $^{208}\text{Pb}/^{204}\text{Pb}$ ratios with respect to the Northern Hemisphere Reference
855 Line (NHRL: Hart, 1984, 1988).

Figure 1

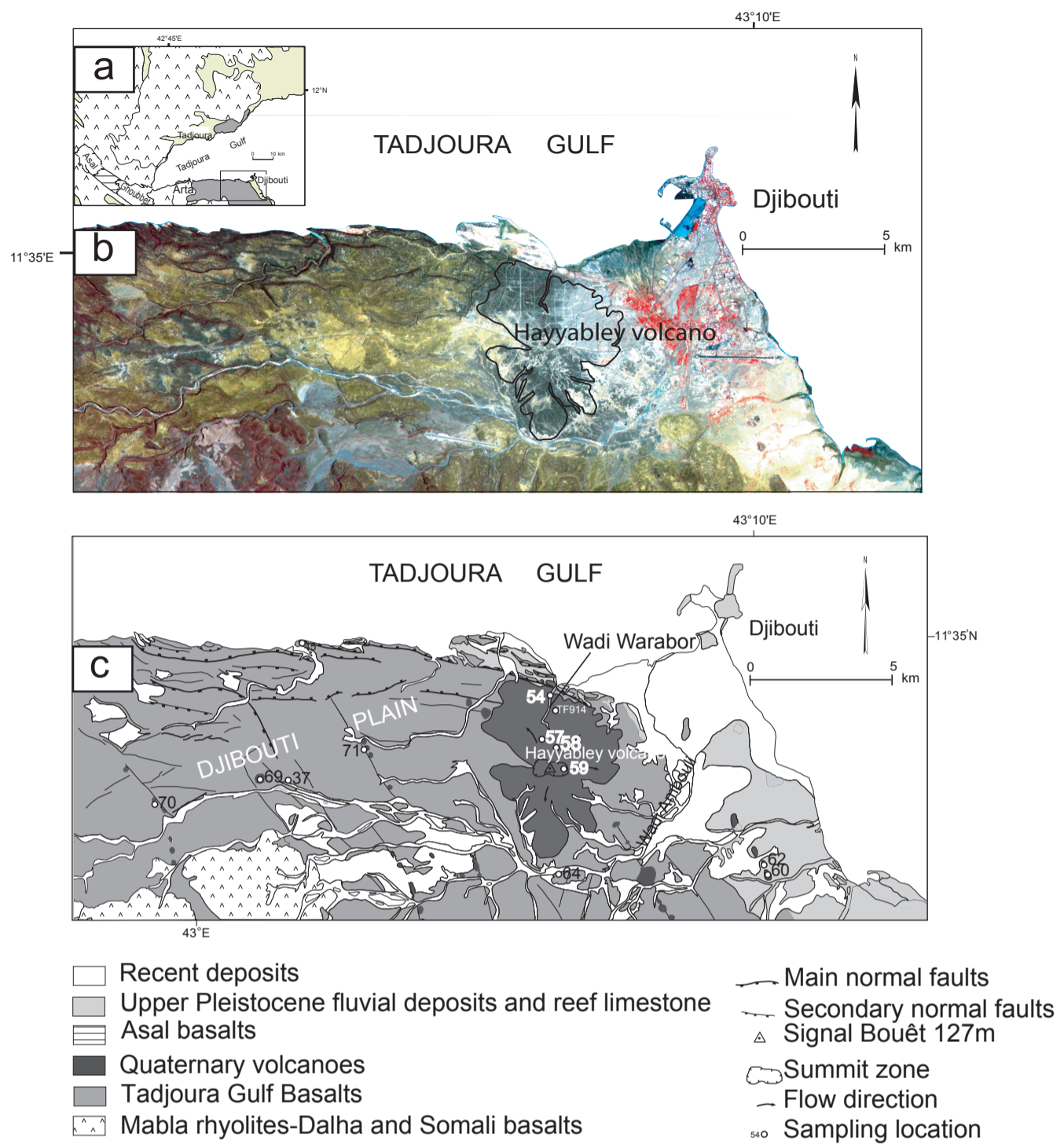


Figure 1: Geology and tectonics of Djibouti Plain

Figure 2

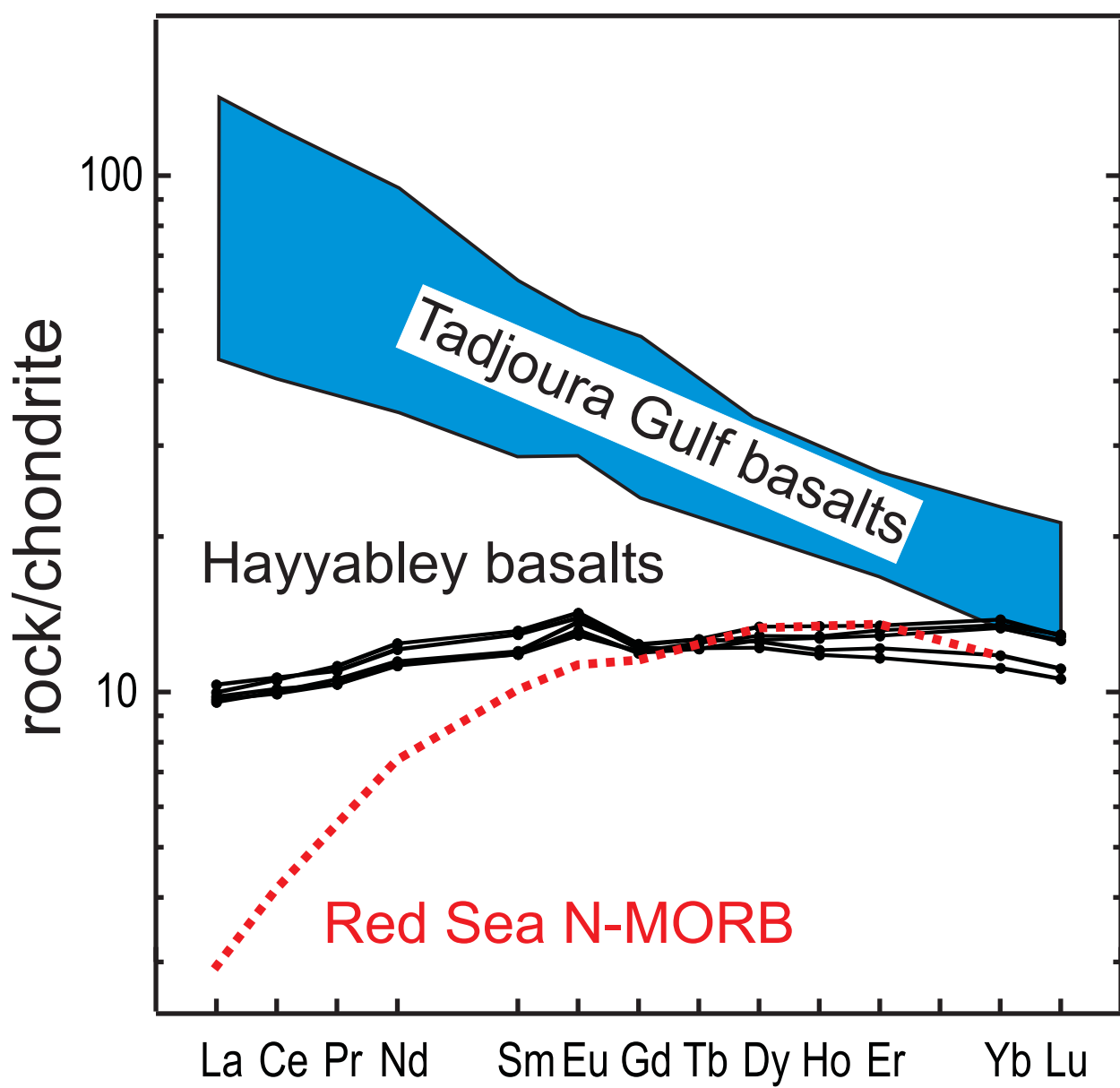


Figure 3

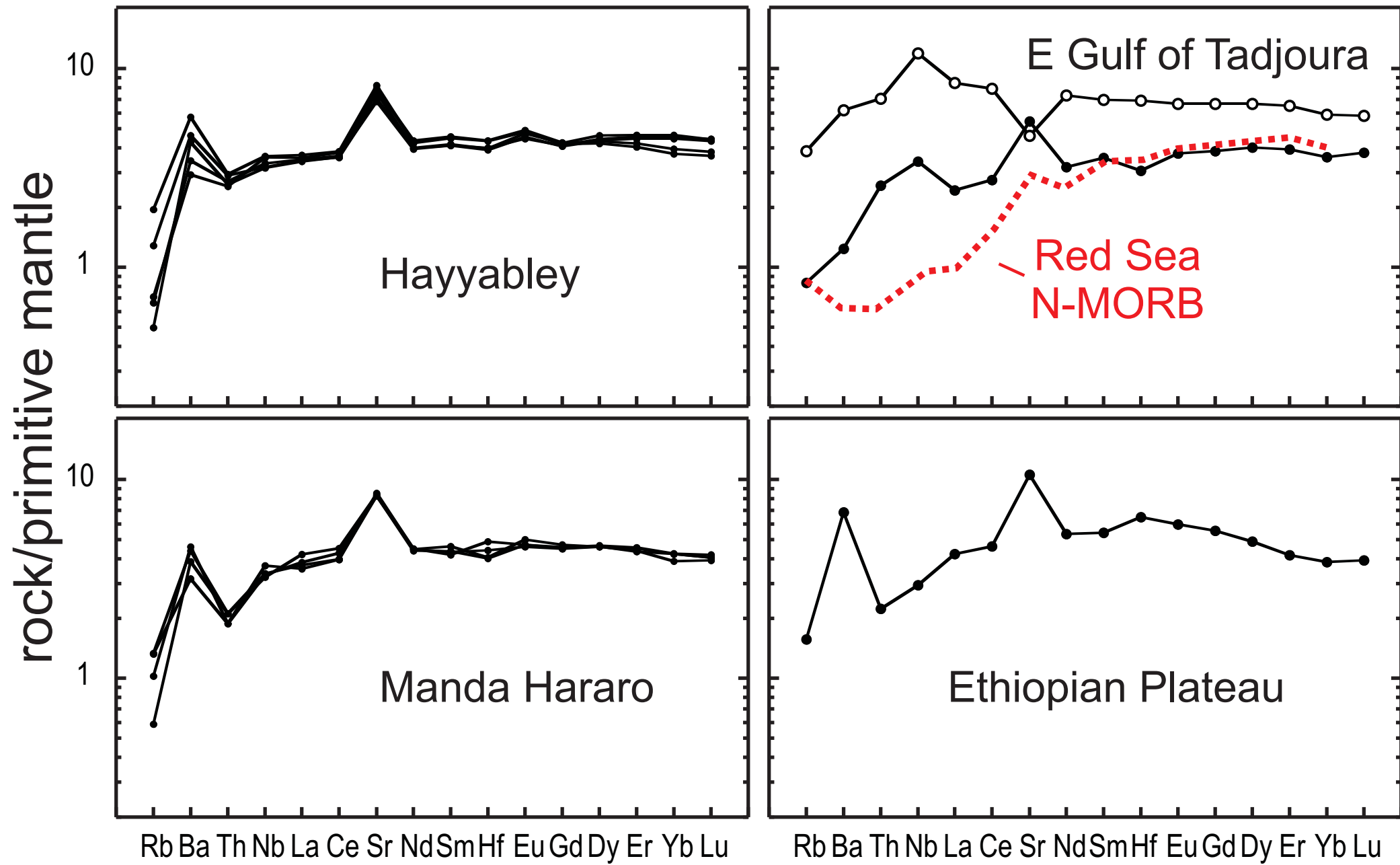


Figure 4

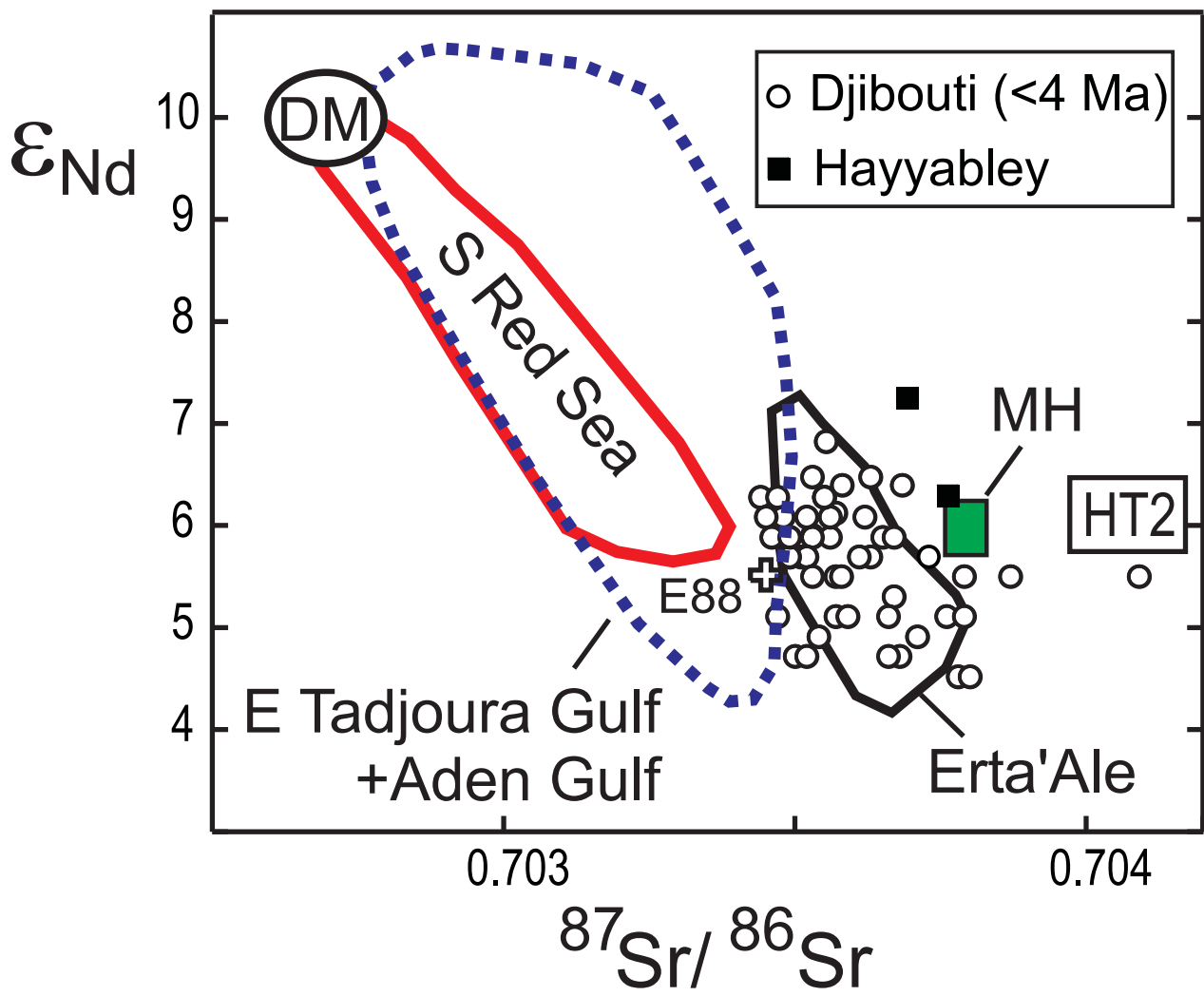


Figure 5

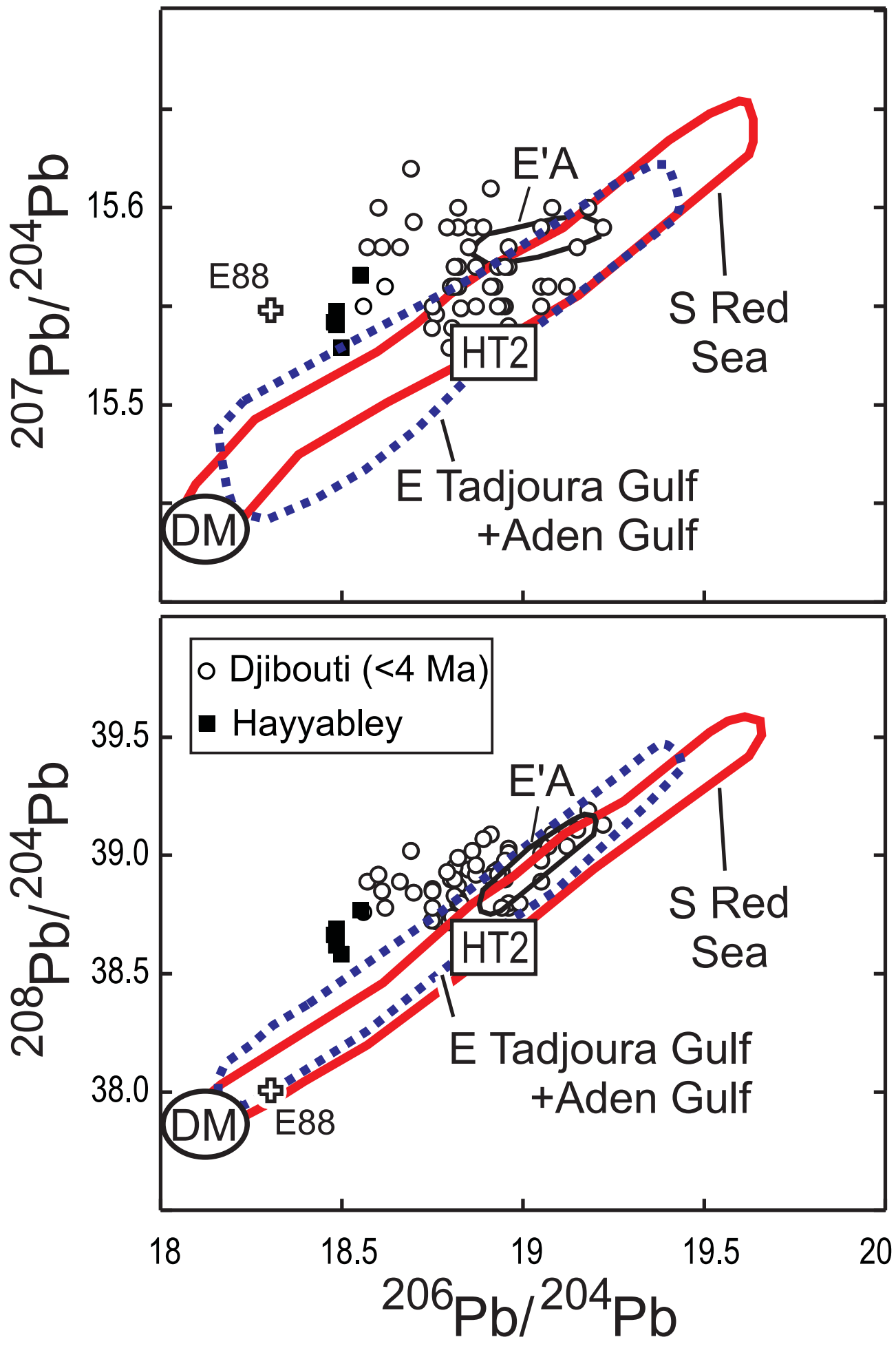


Figure 6

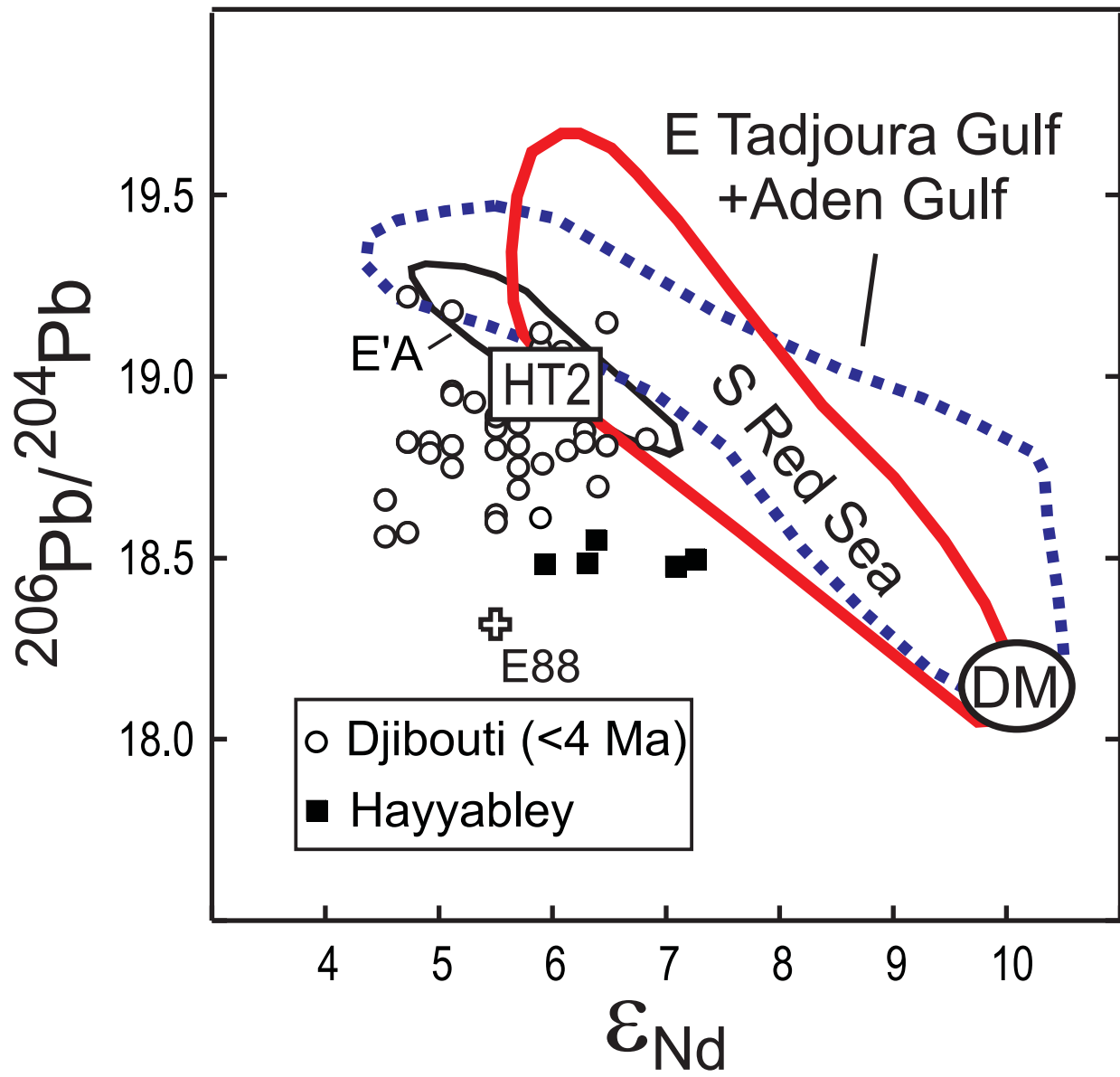


Table 1

[Click here to download Table: Hayya_Table 1nb.doc](#)

1 Table 1. Unspiked ^{40}K - ^{40}Ar datings of Hayyabley basalts. See text for the analytical
 2 procedures.

3

Sample id Experiment #	Split K (wt%) $\pm 1\sigma$	Mass molten (g)	$^{40}\text{Ar}^*\%$	$^{40}\text{Ar}^* 10^{-13}$ (mol./g) $\pm 1\sigma$	Weighted mean $^{40}\text{Ar}^* 10^{-13}$ (mol./g) $\pm 1\sigma$	Age (Ma) $\pm 2\sigma$
DJ54B						
7040	0.09 ± 0.005	2.10972	1.254	1.430 ± 0.057		
7056	« »	2.07428	1.213	1.468 ± 0.058	1.449 ± 0.041	0.93 ± 0.06
DJ54F						
7039	0.04 ± 0.004	2.77642	0.577	0.642 ± 0.046		
7063	« »	3.01844	0.699	0.745 ± 0.040	0.701 ± 0.030	1.06 ± 0.09

4

5 Table 1.

Table 2

[Click here to download Table: Hayy_Table 2nb.doc](#)

- 1 Table 2. Major and trace element analyses of Hayyabley basalts (major oxides in wt%, trace elements in ppm). ICP-AES and ICP-MS analytical
 2 methods described in the text.
 3

	DJ54B	DJ54B	DJ54C	DJ54D	DJ54F	DJ54G	DJ54H	DJ54H	DJ57	DJ57	DJ58	DJ58	DJ59	DJ59
	ICP-AES	ICP-MS	ICP-AES	ICP-AES	ICP-AES	ICP-AES	ICP-AES	ICP-MS	ICP-AES	ICP-MS	ICP-AES	ICP-MS	ICP-AES	ICP-MS
SiO ₂	47.15		47.00	46.8	46.6	46.8	46.5		47.2		46.6		47.6	
TiO ₂	0.93	0.91	0.95	0.95	0.89	0.89	0.91	0.99	0.92	0.90	0.85	0.88	0.96	0.97
Al ₂ O ₃	16.53		16.55	16.40	17.00	16.60	16.50		16.52		16.60		17.05	
Fe ₂ O ₃	11.33		11.50	11.33	11.16	11.22	11.29		11.41		10.29		11.07	
MnO	0.17	0.16	0.17	0.17	0.17	0.16	0.16	0.17	0.17	0.16	0.15	0.14	0.16	0.15
MgO	9.45		8.92	8.75	9.46	9.47	9.30		9.80		9.18		9.25	
CaO	12.90		13.25	13.50	12.50	12.85	13.10		12.90		13.80		12.90	
Na ₂ O	1.99		2.00	1.90	1.98	1.98	1.92		1.96		1.96		2.08	
K ₂ O	0.08		0.07	0.08	0.05	0.09	0.06		0.07		0.1		0.06	
P ₂ O ₅	0.07		0.07	0.07	0.07	0.07	0.07		0.07		0.07		0.07	
LOI	0.46		0.6	0.72	0.63	0.49	0.92		0.05		1.36		-0.38	
Total	101.06		101.08	100.67	100.51	100.62	100.73		101.07		100.96		100.82	
Li		2.77						3.09		2.81		2.67		3.05
Be		0.24						0.26		0.25		0.27		0.29
Sc	45	43.9	46	46	44	44	44	47.4	45	45.5	38	39.6	40	41.1
V	285	266	290	290	275	280	275	291	285	279	245	244	270	253
Cr	380	362	340	340	350	359	355	351	405	388	362	352	370	364
Co	51	52	52	50	53	52	52	55	53	53	48	51	51	51
Ni	198	192	175	175	208	209	198	208	210	201	173	179	175	174
Rb	1.05	0.82	0.8	1	0.5	1	0.85	0.32	0.5	0.42	1.15	1.24	0.5	0.45
Sr	154	149	156	157	155	153	155	160	147	144	174	174	170	168
Y	20.5	20.89	21	20.5	19.5	20	20.5	21.08	20	19.99	17.5	18.49	19	19.57

Zr	48	44.91	48	47	43	46	47	44.09	44	42.81	45	46.87	48	47.77
Nb	2.7	2.28	2.5	2.4	2.5	2.45	2.3	2.26	2.4	2.37	2.6	2.59	2.4	2.56

4 Table 2 (continued).

5

	DJ54B	DJ54B	DJ54C	DJ54D	DJ54F	DJ54G	DJ54H	DJ54H	DJ57	DJ57	DJ58	DJ58	DJ59	DJ59
	ICP-AES	ICP-MS	ICP-AES	ICP-AES	ICP-AES	ICP-AES	ICP-AES	ICP-MS	ICP-AES	ICP-MS	ICP-AES	ICP-MS	ICP-AES	ICP-MS
Ba	34	32.19	41	55	40	50	30	29.81	25	24.11	40	40.01	22	20.49
La	2.6	2.37	2.5	2.4	2.5	2.4	2.5	2.34	2.7	2.40	2.7	2.53	2.5	2.44
Ce	7.1	6.34	7.0	6.5	6.3	6.4	6.7	6.38	6.5	6.47	7.3	6.81	7.0	6.73
Pr		1.00						1.02		1.00		1.06		1.08
Nd	5.3	5.39	5.5	5.3	4.8	5.2	5.4	5.43	5.4	5.34	5.4	5.73	5.8	5.89
Sm	2.0	1.82	2.0	1.7	1.9	1.7	1.8	1.85	1.9	1.82	1.8	1.99	1.9	2.02
Eu	0.8	0.75	0.78	0.78	0.73	0.76	0.77	0.79	0.74	0.76	0.75	0.81	0.82	0.83
Gd	2.3	2.45	2.3	2.4	2.5	2.05	2.4	2.52	2.3	2.43	2.5	2.48	2.5	2.53
Tb		0.47						0.47		0.45		0.46		0.47
Dy	3.3	3.26	3.4	3.3	3.1	3.15	3.25	3.40	3.25	3.21	2.9	3.10	3.25	3.18
Ho		0.73						0.76		0.72		0.67		0.68
Er	2.1	2.19	2.1	2.1	2	2.1	2.15	2.23	2	2.14	1.8	1.93	1.9	2.02
Yb	2.18	2.23	2.29	2.2	2.08	2.1	2.15	2.28	2.1	2.20	1.75	1.84	1.9	1.95
Lu		0.33						0.33		0.32		0.27		0.28
Hf		1.23						1.23		1.21		1.34		1.34
Ta		0.17						0.18		0.18		0.19		0.19
Pb		0.26						0.23		0.26		0.24		0.26
Th		0.25						0.22		0.23		0.25		0.22
U		0.06						0.06		0.05		0.07		0.03

6

7

Table 3. Compositions of light REE depleted basalts from Hayyabley (average of the samples analyzed by ICP-MS), Manda Hararo (average from data given by Barrat et al., 2003), Ethiopian Plateau (sample E88, Pik et al., 1999), and of a N-MORB from Tadjoura Gulf (sample A3D3, Joron et al., 1980; Barrat et al., 1993). (oxides in wt%, traces elements in $\mu\text{g/g}$).

	Hayyabley (n=5)	Manda Hararo (n=4)	Ethiopian Plateau (n=1)	Tadjoura Gulf (n=1)
SiO ₂	47.01	48.50	48.05	48.40
TiO ₂	0.91	1.04	1.08	0.83
Al ₂ O ₃	16.64	15.50	16.05	15.50
Fe ₂ O ₃	11.08	11.94	11.63	9.78
MnO	0.16	0.18	0.17	0.13
MgO	9.40	8.47	8.67	8.83
CaO	13.12	11.32	10.58	12.90
Na ₂ O	1.98	2.33	2.38	2.06
K ₂ O	0.07	0.08	0.16	0.09
P ₂ O ₅	0.07	0.08	0.10	0.05
total	100.93	99.44	98.87	98.57
Sc	43.5	36.7		37.9
V	267	260	229	
Cr	363	64	182	
Co	52.4	54.80		47.7
Ni	191	101	152	139
Rb	0.65	0.68	1.0	0.53
Sr	159	177	224	114.5
Y	20.0	23	21	
Zr	45	41	61	
Nb	2.41	2.43	2.1	
Ba	29.32	28.01	48	8.68
La	2.42	2.63	2.9	1.68
Ce	6.55	7.41	8.2	4.90
Nd	5.56	6.03	7.2	4.33
Sm	1.90	1.94	2.40	1.58
Eu	0.79	0.80	1.00	0.63
Gd	2.48	2.73	3.30	2.30
Dy	3.23	3.40	3.60	2.96
Er	2.10	2.14	2.00	1.88
Yb	2.10	2.04	1.90	1.77
Lu	0.31	0.30	0.29	0.28
Hf	1.27	1.34	2.0	0.95
Ta	0.18	0.18	0.1	0.14
Th	0.23	0.17	0.19	0.18
U	0.05	0.06	0.06	0.28
(La/Sm) _n	0.80	0.85	0.76	0.67
Eu/Eu*	1.11	1.06	1.09	1.01
(Ba/Rb) _n	4.10	3.75	4.36	1.49
(Sr/Ce) _n	2.04	2.01	2.30	1.97

Table 4. Sr, Nd and Pb isotopic compositions for Hayyabley basalts (R: residue after leaching).

	DJ54B	DJ54H	DJ57	DJ58	DJ59
$^{87}\text{Sr}/^{86}\text{Sr}$	0.703909±3	0.703962±5	0.703869±4	0.703871±4	0.703693±5
$^{87}\text{Sr}/^{86}\text{Sr}$ (R)	0.703762±9				
$^{143}\text{Nd}/^{144}\text{Nd}$	0.512961±4	0.513001±3	0.512965±4	0.512942±3	0.513010±4
ϵNd	+6.3	+7.1	+6.4	+5.9	+7.3
$^{206}\text{Pb}/^{204}\text{Pb}$ (R)	18.4856±15	18.4776±15	18.5502±27	18.4842±17	18.4979±21
$^{207}\text{Pb}/^{204}\text{Pb}$ (R)	15.5478±14	15.5421±14	15.5662±25	15.5407±16	15.5292±20
$^{208}\text{Pb}/^{204}\text{Pb}$ (R)	38.6917±43	38.6658±44	38.7692±78	38.6217±50	38.5842±61
$\Delta 7/4$	5.3	4.8	6.4	4.6	3.3
$\Delta 8/4$	71.6	69.9	71.5	64.7	59.3

Table 3

[Click here to download Table: Hayy_Table 3nb.doc](#)

	Hayyabley	Manda	Ethiopian	Tadjoura
		Hararo	Plateau	Gulf
	(n=5)	(n=4)	(n=1)	(n=1)
SiO ₂	47.01	48.50	48.05	48.40
TiO ₂	0.91	1.04	1.08	0.83
Al ₂ O ₃	16.64	15.50	16.05	15.50
Fe ₂ O ₃	11.08	11.94	11.63	9.78
MnO	0.16	0.18	0.17	0.13
MgO	9.40	8.47	8.67	8.83
CaO	13.12	11.32	10.58	12.90
Na ₂ O	1.98	2.33	2.38	2.06
K ₂ O	0.07	0.08	0.16	0.09
P ₂ O ₅	0.07	0.08	0.10	0.05
total	100.93	99.44	98.87	98.57
Sc	43.5	36.7		37.9
V	267	260	229	
Cr	363	64	182	
Co	52.4	54.80		47.7
Ni	191	101	152	139
Rb	0.65	0.68	1.0	0.53
Sr	159	177	224	114.5
Y	20.0	23	21	
Zr	45	41	61	
Nb	2.41	2.43	2.1	
Ba	29.32	28.01	48	8.68
La	2.42	2.63	2.9	1.68
Ce	6.55	7.41	8.2	4.90
Nd	5.56	6.03	<u>7.2</u>	4.33
Sm	1.90	1.94	2.40	1.58
Eu	0.79	0.80	1.00	0.63
Gd	2.48	2.73	3.30	2.30
Dy	3.23	3.40	3.60	2.96
Er	2.10	2.14	2.00	1.88
Yb	2.10	2.04	1.90	1.77
Lu	0.31	0.30	0.29	0.28
Hf	1.27	1.34	2.0	0.95
Ta	0.18	0.18	0.1	0.14
Th	0.23	0.17	0.19	0.18
U	0.05	0.06	0.06	0.28
(La/Sm) _n	0.80	0.85	0.76	0.67
Eu/Eu*	1.11	1.06	1.09	1.01
Ba/Rb	45.11	41.26	48.00	16.38
(Sr/Ce) _n	2.05	2.01	2.30	1.97

1 Table 3. Compositions of LREE-depleted basalts from Hayyabley (average of the samples
2 analysed by ICP-MS), Manda Hararo (average data from Barrat et al., 2003), Ethiopian
3 Plateau (sample E88, Pik et al., 1999), and of a N-MORB from Tadjoura Gulf (sample A3D3,
4 Joron et al., 1980; Barrat et al., 1993). Major oxides in wt%, trace elements in ppm. n denotes
5 ratios normalized to the primitive mantle composition from Sun and McDonough (1989).
6

1 Table 4. Sr, Nd and Pb isotopic compositions of Hayyabley basalts (B: bulk rock; R: residue
 2 after leaching). See text for the analytical procedures. $\Delta 7/4$ and $\Delta 8/4$ denote the deviation (in
 3 ‰) of $^{207}\text{Pb}/^{204}\text{Pb}$ and $^{208}\text{Pb}/^{204}\text{Pb}$ ratios with respect to the Northern Hemisphere Reference
 4 Line (NHRL: Hart, 1984, 1988).

5

	DJ54B	DJ54H	DJ57	DJ58	DJ59
$^{87}\text{Sr}/^{86}\text{Sr}$ (B)	0.703909±3	0.703962±5	0.703869±4	0.703871±4	0.703693±5
$^{87}\text{Sr}/^{86}\text{Sr}$ (R)	0.703762±9				
$^{143}\text{Nd}/^{144}\text{Nd}$ (B)	0.512961±4	0.513001±3	0.512965±4	0.512942±3	0.513010±4
ϵNd	+6.3	+7.1	+6.4	+5.9	+7.3
$^{206}\text{Pb}/^{204}\text{Pb}$ (R)	18.4856±15	18.4776±15	18.5502±27	18.4842±17	18.4979±21
$^{207}\text{Pb}/^{204}\text{Pb}$ (R)	15.5478±14	15.5421±14	15.5662±25	15.5407±16	15.5292±20
$^{208}\text{Pb}/^{204}\text{Pb}$ (R)	38.6917±43	38.6658±44	38.7692±78	38.6217±50	38.5842±61
$\Delta 7/4$	5.3	4.8	6.4	4.6	3.3
$\Delta 8/4$	71.6	69.9	71.5	64.7	59.3

6